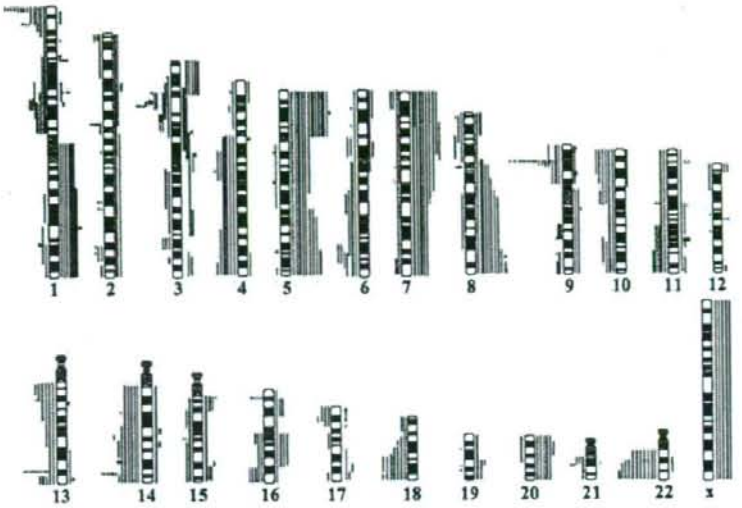

Fig. 2. Summary of chromosome imbalance detected in 17 malignant pleural mesothelioma patients (black lines) and nine cell lines (red lines). Regions of loss and gain are shown by vertical lines on the left (loss) and right (gain) sides of each ideogram. Regions of high-level amplification are presented by thick lines.

line from different individuals, with some shared altered regions being detected. For example, KD1033 (Fig. 1a) and KD1041 (Fig. 1b) showed shared regions including gain of 1p32.1, 5p, 8q, 11q22.1 and 20p and loss of 13q12 and 21q22. Figure 2 is a summary of chromosome imbalance detected in 17 MPM samples (black lines) and nine cell lines (red lines). Regions of high-level gain or amplification (defined as $\log_2$ ratio $> +1.0$) and those of homozygous loss or deletion (defined as $\log_2$ ratio < -1.0) are presented by thick lines. A summary of frequent chromosomal regions of gain and loss, and those of high-level copy gain or amplification, or homozygous loss or deletion detected in 17 MPM samples and nine cell lines is presented in Table 2. We also found that paired samples shared many chromosomal imbalances, although there were several different regions of gains and losses, or regions with relatively weak signals especially in the primary samples. The weak signals were thought to be due to contamination of non-malignant cell DNA (data not shown). Recurrent chromosomal imbalances found in at least six samples consisted of gain on chromosomes 1q (eight tumors/seven individuals), 5p (12/11), 7p (9/8), 8q24 (9/9), 20p (6/6) and loss on chromosomes 1p36.33 (13/13), 1p36.1 (7/7), 1p21.3 (7/6), 3p21.3 (10/8), 4q22 (7/6), 4q34-qter (6/6), 6q25 (7/6), 9p21.3 (16/16), 10p (6/5), 13q33.2 (11/9), 14q32.13 (13/11), 18q (7/6) and 22q (10/8).

High-level gain at 1p32.1 includes *JUN* protooncogene amplification. The array CGH analysis of 26 MPM revealed that 1p32.1 and 11q22.1 were two distinct regions with high-level gains, which were detected in at least two individual samples (Table 2). Interestingly, these high-level gains were observed simultaneously in the two individuals of KD1033 (Fig. 1a) and KD1041 (Fig. 1b). Another sample, KD1039, was also detected for 1p32.1 amplification (data not shown), and KD1039 and KD1041 were derived from the same patient, with the former at the initial surgical resection and the latter at autopsy. Whereas the KD1033 primary tumor showed a larger gain of five consecutive clones at 1p32.1 including the RP11-63G10 clone, KD1039 showed only a gain of the RP11-63G10 clone but not of the neighboring clones, and KD1041 showed only a gain of the two clones RP11-63G10 and RP11-363E22, with RP11-363E22 located toward the centromeric direction from RP11-63G10 1.9 MB apart (data not shown). Thus, the gain of RP11-63G10 seemed to be a very specific, common genetic event for these MPM, and this BAC clone was found to contain the protooncogene *JUN* (Table 2).

Because previous studies have suggested that asbestos fibers induce *JUN* expression in rat pleural mesothelial cells,[42] we studied the *JUN* status of MPM cells in further detail. We carried out Southern blot analysis with nine primary tumors and nine cell lines, and confirmed *JUN* high-level amplification in the three samples but not in the remaining 15 samples (Fig. 3a). To determine whether these MPM overexpress the transcripts of *JUN*, we carried out quantitative real-time PCR with 11 MPM samples available for RNA analysis together with seven MPM cell lines and one non-malignant mesothelial cell line, MeT-5 A. We found that KD1041, with high-level amplification of *JUN*, overexpressed mRNA of *JUN* (Fig. 3b). Interestingly, we noticed that there seemed to be three groups with distinct levels of *JUN* expression. We classified MPM into three groups according to the levels of *JUN* expression: high-level expresser (defined as >0.15) for three tumors (KD977, KD1041 and KD1044), middle-level expresser (defined as $0.025 < JUN < 0.15$) for eight tumors (KD1032, KD1033, KD1045, KD1046, KD1048, KD1049, ACC-MESO-4 and H290), and low-level expresser (defined as <0.025) for seven tumors (KD471, KD476, ACC-MESO-1, Y-MESO-8A, Y-MESO-8D, H28 and MSTO-211H) and MeT-5 A. Among the seven MPM cell lines, ACC-MESO-4 and H290 were classified into middle-level expresser and the remaining five into low-level expressers. We also studied the *FOS* expression to determine whether *JUN* coexpresses with *FOS* in MPM cells (Fig. 3c). Most of the MPM cells classified into either high- or middle-level expresser of *JUN* simultaneously expressed *FOS* equal or greater than 0.025, and most expressers of both genes were primary tumors.

Alterations of *p16^{INK4a}/p14^{ARF}* at 9p21.3 and *NF2* at 22q12.2. We found frequent deletions of RP11-149I2 located at 9p21.3 in seven MPM samples and nine MPM cell lines, with five samples (two primary tumors and three cell lines) showing high-level loss. This BAC clone included *p16^{INK4a}/p14^{ARF}*, which is one of the most frequently mutated TSG in human malignancies, and we showed previously that *p16^{INK4a}/p14^{ARF}* was deleted in all MPM cell lines studied.[28] To determine whether the 9p21 deletion region in MPM extends further beyond the *p16^{INK4a}/p14^{ARF}* gene locus, which may indicate another target TSG of MPM in this region, we further carried out PCR analysis using multiple primer sets for comparison with locations of BAC and PAC clones on 9p21. Besides the nine MPM cell lines, another three MPM cell lines (NCI-H290, NCI-H513 and NCI-H2373) were also studied.

Table 2. Chromosomal regions with frequent imbalances or high copy gain or loss detected in malignant pleural mesothelioma

Alteration	Chromosomal region	No. patients (n = 17)	No. cell lines (n = 9)	No. individuals (n = 22)	Gene†	BAC/PAC‡
Gain						
	1p32.1§	3	0	2	*JUN*	RP11-63G10
	1q	4	4	7		
	5p	8	4	11	*CDH10*	RP11-116O11
	7p	5	4	8		
	8q24	4	5	9	*MYC*	RP1-80K22
	11q22.1§	2	0	2	*IAP*	RP11-864G5
	20p	3	3	6		
Loss						
	1p36.33	12	1	13	*KIT*	RP11-181G12
	1p36.1	4	3	7	*NM_018125*	RP11-473A10
	1p21.3	2	5	6	*RPL5*	RP4-716F6
	3p21.3	7	3	8	*PFKFB4*	RP5-1034C16
	4q22	2	5	6	*TMSL3*	RP11-309H6
	4q34-qter	3	3	6	*Q9P2F5*	RP11-739P1
	6q25	3	4	6	*PLEKHG1*	RP11-291C6
	9p21.3§	7	9	16	$p16^{INK4a}/p14^{ARF}$	RP11-149I2
	10p	2	4	5		
	13q33.2	7	4	9	*DAOA*	RP11-166E2
	14q32.13	8	5	11	*CHGA/ITPK1*	RP11-862G15
	18q	4	3	6	*MALT1*	RP11-4G8
	22q	7	3	8	*NF2*	RP1-76B20

†Representative genes are listed at each region when bacterial artificial chromosome (BAC) and P-1-derived artificial chromosome (PAC) clones of continuously ordered gain or loss of maximum overlapped clones were less than 10, when known protooncogenes or tumor suppressor genes shown to be involved in human malignancies were located, or when only a few genes were located in this region. ‡A representative BAC/PAC clone was listed when continuously ordered gain or loss of maximum overlapped region was less than 10 clones, and the clone at the mid-point of the overlapped region was chosen. §High copy gain or loss was observed.

After we confirmed homozygous deletions of exons 1, 2 and 3 of the $p16^{INK4a}$ gene and exon 1β of the $p14^{ARF}$ gene in all 12 (100%) MPM cell lines except MSTO-211H, which showed a partial retention of the gene, we used 16 microsatellite markers and one sequence site-tagged marker for the analysis (Fig. 4). For the telomeric direction, the INF-α cluster of genes was homozygously deleted in two cell lines but not in the remaining 10. For the centromeric direction, two cell lines (NCI-H290 and H2052) showed a larger deletion with consecutive losses at markers including D9S259, suggesting that these two cell lines had at least 4 Mb homozygous deletion. Meanwhile, four cell lines (Y-MESO-8A, -8D, NCI-H28 and H513) had a smaller homozygous deletion that was limited within D9S1749 and D9S790, suggesting that the maximum deletion size was less than 482 kb.

Finally, we studied any point mutations of the *NF2* gene in 17 primary tumors. After sequencing 17 exons covering the entire coding region of *NF2*, we found that three tumors had small deletions, all of which resulted in a frameshift mutation (Table 1). Because genomic DNA extracted from snap-frozen primary tumor tissues was used for the analysis, the existence of homozygous deletion was not determined due to possible contamination of non-cancerous DNA.

Discussion

In the present study, we analyzed 17 MPM primary tumors and nine MPM cell lines using array CGH and identified regions of genomic gain and loss. Regions of genomic aberrations observed in >20% of individuals were 1q, 5p, 7p, 8q24 and 20p with gains, and 1p36.33, 1p36.1, 1p21.3, 3p21.3, 4q22, 4q34-qter, 6q25, 9p21.3, 10p, 13q33.2, 14q32.13, 18q and 22q with losses. We confirmed the same chromosomal alterations as reported earlier by other groups and further identified high gain or amplification regions including 1p32, which harbors the *JUN* protooncogene. To our knowledge, our present study provides the first detailed array CGH data on chromosomal imbalances in MPM patient tumors and cell lines.

Traditional allelotyping and karyotype analyses revealed nonrandom chromosomal abnormalities including 1p, 3p, 4p15.1-p15.3, 4q25-q26, 4q33-q34, 6q, 9p, 14q11.1-q12, 14q23-q24 and 22q.[11–18,43,44] Subsequently, chromosomal CGH (also known as conventional CGH) has been carried out to detect more detailed abnormalities in MPM (Table 3). For example, Krismann *et al.* showed a total of 77 cases of MPM in the main histological subtypes (epithelioid type, sarcomatoid type and biphasic type) using chromosomal CGH.[34] They reviewed common gains at the chromosomal regions of 1q23/1q32, 7p14-p15, 8q22-q23 and 15q22-q25, and common losses at the chromosomal regions of 1p21, 3p21, 4p12-p13, 4q31-q32, 6q22, 9p21, 10p13-pter, 13q13-q14, 14q12-q24, 17p12-pter and 22q in all subtypes. In the present study with array CGH analysis, we also detected similar aberrations of multiple loci that have been found in previous studies.[29–35] These regions include gains of 1p32, 1q and 7p, and losses of 1p21, 9p21 and 22q. In addition to these regions, we have identified new regions such as 8q24 and 13q33.2, which had not been detected with chromosomal CGH analysis. The gain of 8q24 locus was detected by array CGH in nine cases (nine individuals) of these 26 samples. A single BAC, RP1-80K22, which includes the known protooncogene *MYC*, was located at the overlapped regions of 8q24 amplification. As a previous study showed a significant increase in signal strength of *MYC* in the mesothelioma tissues from an experimental animal model, compared with basal expression in non-neoplastic mesothelial cells, our findings also support the importance of *MYC* alteration in the development of MPM.[45]

Previous reports of chromosomal CGH analysis of MPM samples identified the region of gain at 1p32, although a specific candidate target gene was not referred to in detail.[34,46] Using array CGH, we found that a single BAC clone, RP11-63G10,

doi: 10.1111/j.1349-7006.2006.00386.x

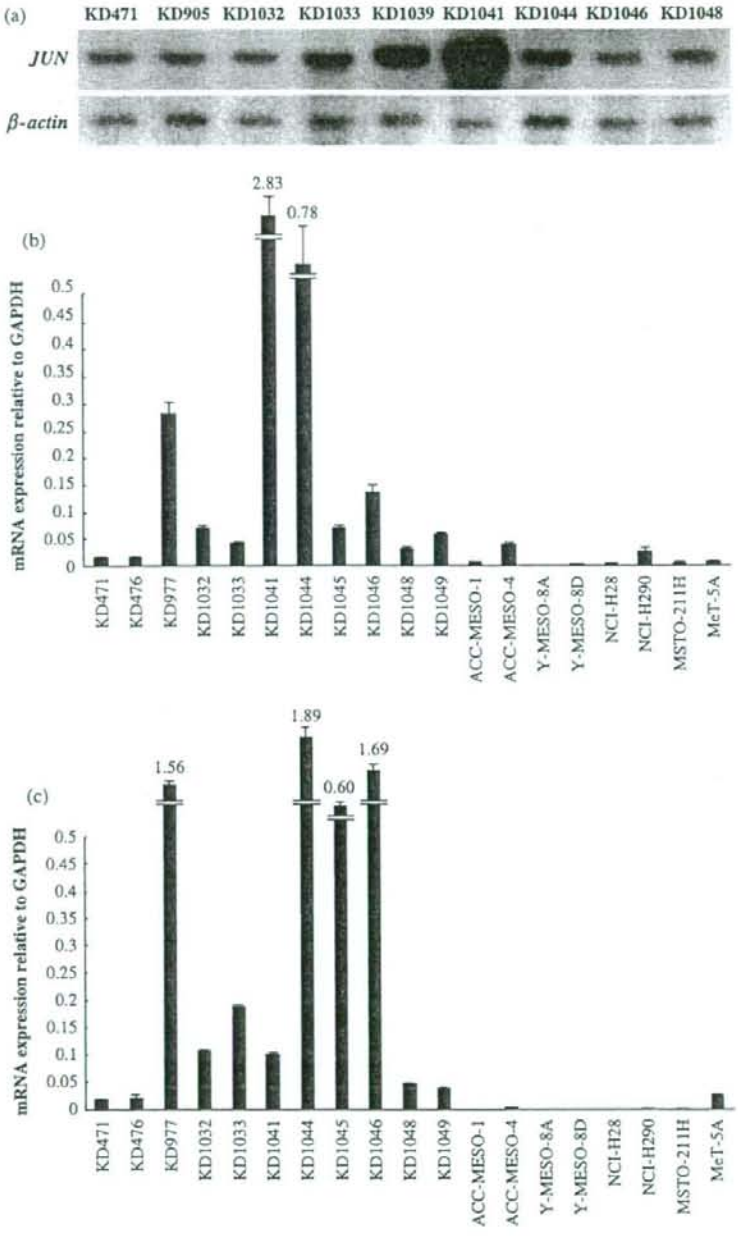

Fig. 3. *JUN* amplification at 1p32.1 and expression of *JUN* and *FOS* messages in malignant pleural mesothelioma. (a) Southern blot analysis of *JUN*. Each lane was loaded with 7 μg genomic DNA from MPM samples. Southern blot shows high-level amplification of *JUN* in KD1039 and KD1041 and low-level amplification in KD1033. (b,c) Diagrammatic presentation of quantitative real-time polymerase chain reaction data for (b) JUN and (c) FOS mRNA from 11 primary samples, seven MPM cell lines and MeT-5 A. The results were averages of at least three independent experiments with error bars showing standard deviations. MPM were classified into three groups of JUN status expression: high-level expresser (defined as >0.15) for three tumors (KD977, KD1041 and KD1044), middle-level expresser (defined as 0.025 < *JUN* < 0.15) for eight tumors (KD1032, KD1033, KD1045, KD1046, KD1048, KD1049, ACC-MESO-4 and H290), and low-level expresser (defined as <0.025) for the remaining seven tumors and MeT-5A. MPM were also classified into three groups according to *FOS* expression status: high-level expresser (defined as >0.15) for five tumors (KD977, KD1033, KD1044, KD1045 and KD1046), middle-level expresser (defined as 0.025 < *FOS* < 0.15) for four tumors (KD1032, KD1041, KD1048 and KD1049) and MeT-5 A, and low-level expresser (defined as <0.025) for the remaining nine tumors.

detected the region of gain at 1p32.1 in three tumors from two individuals. The RP11-63G10 clone was the only clone that showed overlapping at this region, and harbored only one known gene, the *JUN* protooncogene. Whereas KD1033 showed relatively wide-range amplification including five consecutive clones, KD1039 and KD1041 showed only RP11-63G10 amplification or with another neighbor clone for the latter (data not shown). It is noteworthy that KD1039 and KD1041 were from the same patient at surgical resection and autopsy, respectively, but the ranges of amplification of the *JUN* locus were slightly different. Furthermore, except for 1p32, these two samples also showed distinct regions of chromosomal alteration for each locus, including a gain at 13q34 for KD1039, and gains at 11p15.2 and 11q22.1 and a loss at 13q33.2 for KD1041 (data not shown). Although we confirmed the identity of these two samples with 16 STR repeats, it remains unclear whether the KD1041 cells originated from a subclonal cancer cell population that existed in the KD1039 tumor and acquired another chromosomal alteration during propagation.

JUN is a transcription factor and functions through homodimerization or heterodimerization with FOS to form the transcription factor AP-1, which can bind to the promoter region of

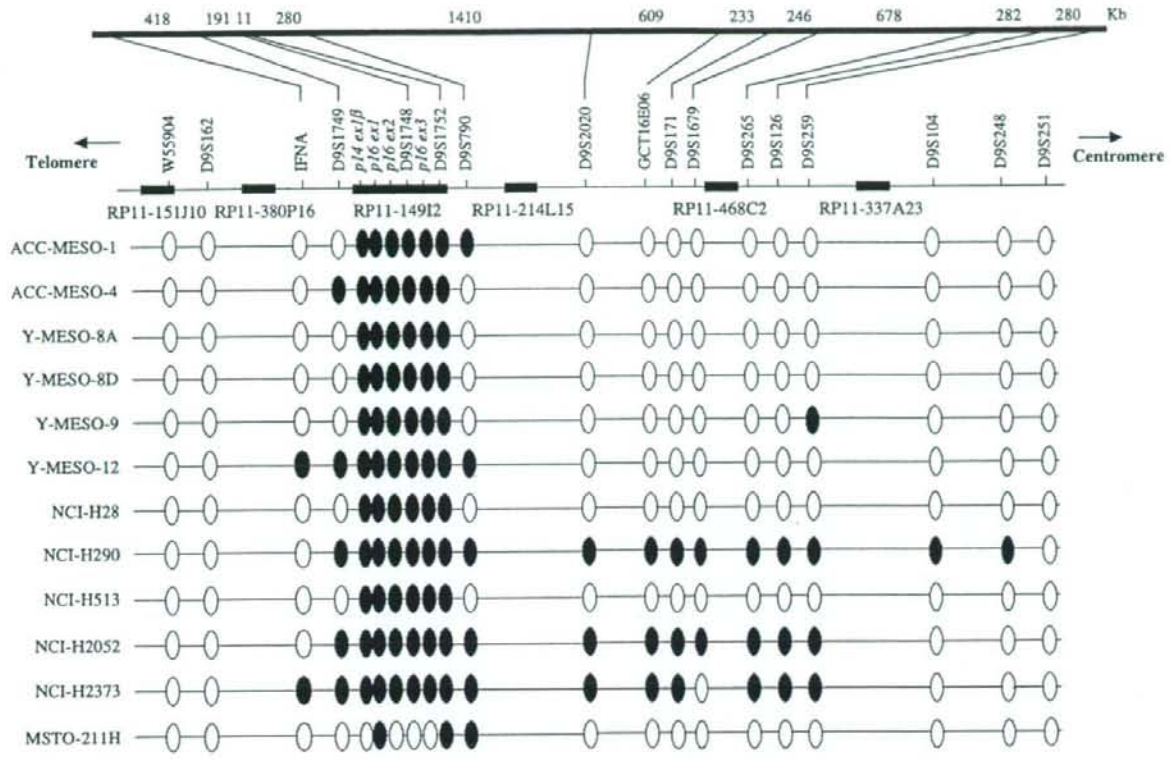

Fig. 4. Homozygous deletion map of the 9p21 region in 12 malignant pleural mesothelioma cell lines. Results of polymerase chain reaction analysis for each locus are shown by open ovals (retention) and closed ovals (homozygous deletion). Locations of genes and markers are according to those of the GDB Human Genome Database and Ensembl Genome Browser. Top bar shows the sizes between the selected markers proportionally: W55904 – (570 kb) – D9S162–(1.71 Mb) – IFNA – (418 kb) – D9S1749 – (191 kb) – D9S1748–(11 kb) – D9S1752 – (280 kb) – D9S790 – (1.41Mb) – D9S2020 – (609 kb) – GCT16E06 – (233 kb) – D9S171 – (246 kb) – D9S1679–(678 kb) – D9S265–(282 kb) – D9S126 – (280 kb) – D9S259 – (2.75 Mb) – D9S104 – (1.15 Mb) – D9S248 – (898 kb) – D9S251.

Table 3. Chromosomal regions with frequent imbalances shown in malignant pleural mesotheliomas from previous reports using chromosomal comparative genomic hybridization (CGH), and the current study using genome-wide array-based CGH

Authors	Year	Samples	Frequent gains	Frequent losses
Kivipensas *et al.*	1996	11	5p, 6p, 8q, 15q, 17q, 20	1p, 8p, 14q, 22q
Bjorkqvist *et al.*	1997	27	1cen-qter	4q31.1-qter, 6q22-q24, 9p21-pter, 13, 14q24-qter, 22q13
Bjorkqvist *et al.*	1998	34	7p, 15q	4q, 6q, 14q
Balsara *et al.*	1999	24	5p	1p12-p22, 6q25-qter, 9p21, 13q12-q14, 14q24-qter, 15q11.1-q15, 22q
Krismann *et al.*	2002	77	1q23/1q32, 7p14-p15, 8q22-q23, 15q22-q25	1p21, 3p21, 4p12-p13, 4q31-q32, 6q22, 9p21, 10p13-pter, 13q13-q14, 14q12-q24, 17p12-pter, 22q
Current study		26	1q, 5p, 7p, 8q24, 20p	1p36.33, 1p36.1, 1p21.3, 3p21.3, 4q22, 4q34-qter, 6q25, 9p21.3, 10p, 13q33.2, 14q32.13, 18q, 22q

intermediate genes involved in cell division and other cell functions.[47] Heintz *et al.* reported that both crocidolite and chrysotile asbestos caused increases in the expression of *JUN* and *FOS* in rat pleural mesothelial cells.[42] They demonstrated that, in contrast to phorbol 12-myristate 13-ester, which induced rapid and transient increases in *JUN* and *FOS* mRNA, asbestos caused 2–5-fold increases in *JUN* and *FOS* mRNA dose-dependently, which persisted for at least 24 h in mesothelial cells. They concluded that by activating the early response gene pathway, asbestos may induce chronic cell proliferation that subsequently contributes to carcinogenesis in lung and pleura. Thus, our findings of *JUN* amplification and overexpression detected in MPM tumors is very intriguing, and we also found that three tumors with *JUN* amplification were from patients with high-grade asbestos exposure. Interestingly, five of seven MPM cell lines were classified into low-level expressers of *JUN*, compared with three high-level and six middle-level expressers of the 11 primary tumors. This finding suggests that primary MPM tumor cells are

doi: 10.1111/j.1349-7006.2006.00386.x

continuously exposed to some stress to induce *JUN* transcription, and that *JUN* transcription is not necessarily induced in the established MPM cell line and MeT-5 A cells under usual tissue culture conditions, which may also indicate that the levels detected in MPM cell culture are of baseline *JUN* expression. Meanwhile, the analysis of *FOS* expression revealed that it was expressed simultaneously with *JUN* in most MPM cases, with high levels of expression of both genes detected mainly in the primary tumors, but not in cell cultures. These findings suggest the possibility that some surgical manipulations cause artificial induction of some genes, including early response genes,[48] which leads to the observation of predominant expression of these genes in the primary tumors. Nevertheless, because gene amplification of *JUN* was indeed identified in three MPM tumors, we think that there were some strong and persistent factors for *JUN* activation during the development of the MPM tumor cells.

JUN has been shown to be induced by other factors such as hypoxia. A recent immunohistochemical analysis detected expression of hypoxia-inducible factor 1α at focal regions in most MPM tumors but not in mesothelial cells, suggesting that hypoxic stress exists in primary MPM tumors.[49] Although the mechanisms and causes of amplification of genes such as *MYC* family members remain poorly understood, amplification of several other genes has been implicated as being induced by carcinogens and other stresses, such as amplification of the dihydrofolate reductase gene via methotrexate treatment.[50] Thus, we speculate that the chronic induction of *JUN* expression might have been induced by multiple stimuli, most importantly by asbestos fibers at the initial stage and possibly by hypoxia and other unidentified factors continuously, and that this might result in gene amplification of *JUN* in a subset of MPM cells during long latency.

Using array CGH, we found a region of loss at 9p21 in 16 tumors (16 individuals) that was covered by a single BAC clone, RP11-149I2, which included the $p16^{INK4a}/p14^{ARF}$ gene. It is well known that $p16^{INK4a}/p14^{ARF}$ is one of the most frequently deleted genes in many types of human cancers. Previous studies by other groups identified frequent alteration of $p16^{INK4a}/p14^{ARF}$ in most MPM, and we have also shown that $p16^{INK4a}/p14^{ARF}$ was deleted in all 10 MPM cell lines studied.[28] Although studies with simple PCR techniques reported homozygous deletion of $p16^{INK4a}/p14^{ARF}$ at a relatively lower frequency in MPM tissues than in cell lines, which may be due to contamination of a significant amount of normal stromal cells, we detected frequent deletion at 9p21.3 in seven MPM samples with array CGH. Furthermore, we determined the approximate lengths of deletion regions in 12 MPM cell lines, compared with the locations of DNA markers and BAC or PAC clones. We found that several cell lines showed a relatively small deletion with a maximum deletion size of 482 kb, whereas others showed at least a 4-Mb deletion size. Our findings of the $p16^{INK4a}/p14^{ARF}$ deletion in MPM seem consistent with other reports that the sizes of homozygous deletions vary individually in any given tissue type of malignancy.[51–53] Although it is very clear that $p16^{INK4a}/p14^{ARF}$ is the most important target TSG at the 9p21.3 region, other genes in this homozygous deletion region should also be studied to determine whether any of them play a role in the development of MPM.

Finally, the loss of 3p21.3 locus was detected by array CGH in 10 cases (eight individuals) of the 26 samples. One of the well-known TSG located at this region is *RASSF1A*, which is frequently inactivated by promoter hypermethylation in various types of human malignancies. The frequent hypermethylation of *RASSF1A* was also reported in MPM, which suggests that *RASSF1A* is a strong target TSG at 3p21 during the development of MPM.[54] Meanwhile, we also identified a homozygous deletion including *CTNNB1* (β-catenin) at 3p22.1 in the NCI-H28 cell line, and further demonstrated that the exogenously transfected *CTNNB1* gene inhibited the growth of NCI-H28 cells.[55,56] Thus, because several genes have been suggested as candidate TSG at the 3p21-22 region for various malignancies including MPM, further detailed analysis may be warranted to clarify the most important target TSG in this region for MPM.

To summarize, we subjected MPM samples to array CGH analysis and found genomic regions altered recurrently in MPM, including 1p32 *JUN* protooncogene amplification. Array CGH analysis can thus be expected to provide new insights into the genetic background of MPM and to offer some clues to developing a new molecular target therapy for this highly aggressive fatal tumor.

Acknowledgments

This work was supported by a Grant-in-Aid for Scientific Research from the Japan Society for the Promotion of Science. We would like to thank Dr Adi F. Gazdar for the cell lines, and Dr Yutaka Kondo, Dr Hirotaka Osada, Dr Masashi Kondo and Dr Toshimichi Yamamoto for helpful comments and special encouragement.

References

1 Whitaker D, Papadimitriou JM, Walters MN. The mesothelium and its reactions: a review. *Crit Rev Toxicol* 1982; **10**: 81–144.
2 Lanphear BP, Buncher CR. Latent period for malignant mesothelioma of occupational origin. *J Occup Med* 1992; **34**: 718–22.
3 Carbone M, Kratzke RA, Testa JR. The pathogenesis of mesothelioma. *Semin Oncol* 2002; **29**: 2–17.
4 Pass HI, Vogelzang N, Hahn S, Carbone M. Malignant pleural mesothelioma. *Curr Probl Cancer* 2004; **28**: 93–174.
5 Peto J, Decarli A, La Vecchia C, Levi F, Negri E. The European mesothelioma epidemic. *Br J Cancer* 1999; **79**: 666–72.
6 Robinson BW, Lake RA. Advances in malignant mesothelioma. *N Engl J Med* 2005; **353**: 1591–603.
7 Murayama T, Takahashi K, Natori Y, Kurumatani N. Estimation of future mortality from pleural malignant mesothelioma in Japan based on an age-cohort model. *Am J Ind Med* 2006; **49**: 1–7.
8 Curran D, Sahmoud T, Therasse P, van Meerbeeck J, Postmus PE, Giaccone G. Prognostic factors in patients with pleural mesothelioma: the European Organization for Research and Treatment of Cancer experience. *J Clin Oncol* 1998; **16**: 145–52.
9 van Meerbeeck JP, Gaafar R, Manegold C *et al*. Randomized phase III study of cisplatin with or without raltitrexed in patients with malignant pleural mesothelioma: an intergroup study of the European Organisation for Research and Treatment of Cancer Lung Cancer Group and the National Cancer Institute of Canada. *J Clin Oncol* 2005; **23**: 6881–9.
10 Vogelzang NJ, Rusthoven JJ, Symanowski J *et al*. Phase III study of pemetrexed in combination with cisplatin versus cisplatin alone in patients with malignant pleural mesothelioma. *J Clin Oncol* 2003; **21**: 2636–44.
11 Gibas Z, Li FP, Antman KH, Bernal S, Stahel R, Sandberg AA. Chromosome changes in malignant mesothelioma. *Cancer Genet Cytogenet* 1986; **20**: 191–201.
12 Popescu NC, Chahinian AP, DiPaolo JA. Nonrandom chromosome alterations in human malignant mesothelioma. *Cancer Res* 1988; **48**: 142–7.
13 Tiainen M, Tammilehto L, Mattson K, Knuutila S. Nonrandom chromosomal abnormalities in malignant pleural mesothelioma. *Cancer Genet Cytogenet* 1988; **33**: 251–74.
14 Flejter WL, Li FP, Antman KH, Testa JR. Recurring loss involving chromosomes 1, 3, and 22 in malignant mesothelioma: possible sites of tumor suppressor genes. *Genes Chromosomes Cancer* 1989; **1**: 148–54.
15 Hagemeijer A, Versnel MA, Van Drunen E *et al*. Cytogenetic analysis of malignant mesothelioma. *Cancer Genet Cytogenet* 1990; **47**: 1–28.
16 Taguchi T, Jhanwar SC, Siegfried JM, Keller SM, Testa JR. Recurrent deletions of specific chromosomal sites in 1p, 3p, 6q, and 9p in human malignant mesothelioma. *Cancer Res* 1993; **53**: 4349–55.
17 Lee WC, Balsara B, Liu Z, Jhanwar SC, Testa JR. Loss of heterozygosity analysis defines a critical region in chromosome 1p22 commonly deleted in human malignant mesothelioma. *Cancer Res* 1996; **56**: 4297–301.
18 Bell DW, Jhanwar SC, Testa JR. Multiple regions of allelic loss from chromosome arm 6q in malignant mesothelioma. *Cancer Res* 1997; **57**: 4057–62.
19 Cheng JQ, Jhanwar SC, Klein WM *et al*. p16 alterations and deletion mapping of 9p21-p22 in malignant mesothelioma. *Cancer Res* 1994; **54**: 5547–51.

20 Xio S, Li D, Vijg J, Sugarbaker DJ, Corson JM, Fletcher JA. Codeletion of p15 and p16 in primary malignant mesothelioma. *Oncogene* 1995; **11**: 511–15.
21 Sekido Y, Pass HI, Bader S *et al.* Neurofibromatosis type 2 (NF2) gene is somatically mutated in mesothelioma but not in lung cancer. *Cancer Res* 1995; **55**: 1227–31.
22 Bianchi AB, Mitsunaga SI, Cheng JQ *et al.* High frequency of inactivating mutations in the neurofibromatosis type 2 gene (NF2) in primary malignant mesotheliomas. *Proc Natl Acad Sci USA* 1995; **92**: 10854–8.
23 Murthy SS, Testa JR. Asbestos, chromosomal deletions, and tumor suppressor gene alterations in human malignant mesothlioma. *J Cell Physiol* 1999; **180**: 150–7.
24 Jaurand MC, Fleury-Feith J. Pathogenesis of malignant pleural mesothelioma. *Respirology* 2005; **10**: 2–8.
25 Metcalf RA, Welsh JA, Bennett WP *et al.* p53 and Kirsten-ras mutations in human mesothelioma cell lines. *Cancer Res* 1992; **52**: 2610–15.
26 Papp T, Schipper H, Pemsel H *et al.* Mutational analysis of N-ras, p53, 16INK4a, p14ARF and CDK4 genes in primary human malignant mesotheliomas. *Int J Oncol* 2001; **18**: 425–33.
27 Kumar K, Rahman Q, Schipper H, Matschegewski C, Schiffmann D, Papp T. Mutational analysis of 9 different tumour-associated genes in human malignant mesothelioma cell lines. *Oncol Rep* 2005; **14**: 743–50.
28 Usami N, Fukui T, Kondo M *et al.* Establishment and characterization of four malignant pleural mesothelioma cell lines from Japanese patients. *Cancer Sci* 2006; **97**: 387–94.
29 Kivipensas P, Bjorkqvist AM, Karhu R *et al.* Gains and losses of DNA sequences in malignant mesothelioma by comparative genomic hybridization. *Cancer Genet Cytogenet* 1996; **89**: 7–13.
30 Bjorkqvist AM, Tammilehto L, Anttila S, Mattson K, Knuutila S. Recurrent DNA copy number changes in 1q, 4q, 6q, 9p, 13q, 14q and 22q detected by comparative genomic hybridization in malignant mesothelioma. *Br J Cancer* 1997; **75**: 523–7.
31 Bjorkqvist AM, Tammilehto L, Nordling S *et al.* Comparison of DNA copy number changes in malignant mesothelioma, adenocarcinoma and large-cell anaplastic carcinoma of the lung. *Br J Cancer* 1998; **77**: 260–9.
32 Balsara BR, Bell DW, Sonoda G *et al.* Comparative genomic hybridization and loss of heterozygosity analyses identify a common region of deletion at 15q11.1-15 in human malignant mesothelioma. *Cancer Res* 1999; **59**: 450–4.
33 De Rienzo A, Testa JR. Recent advances in the molecular analysis of human malignant mesothelioma. *Clin Ther* 2000; **151**: 433–8.
34 Krismann M, Müller KM, Jaworska M, Johnen G. Molecular cytogenetic differences between histological subtypes of malignant mesotheliomas: DNA cytometry and comparative genomic hybridization of 90 cases. *J Pathol* 2002; **197**: 363–71.
35 Sambrook J, Fritsch EF, Maniatis T. *Molecular Cloning: A Laboratory Manual*. Cold Spring Harbor, NY: Cold Spring Harbor Laboratory Press, 1989.
36 Tagawa H, Karnan S, Suzuki R *et al.* Genome-wide array-based CGH for mantle cell lymphoma: identification of homozygous deletions of the proapoptotic gene BIM. *Oncogene* 2005; **24**: 1348–58.
37 Pinkel D, Segraves R, Sudar D *et al.* High resolution analysis of DNA copy number variation using comparative genomic hybridization to microarrays. *Nat Genet* 1998; **20**: 207–11.
38 Ota A, Tagawa H, Karnan S *et al.* Identification and characterization of a novel gene, C13orf25, as a target for 13q31-q32 amplification in malignant lymphoma. *Cancer Res* 2004; **64**: 3087–95.
39 Karnan S, Tsuzuki S, Kiyoi H *et al.* Genomewide array-based comparative genomic hybridization analysis of acute promyelocytic leukemia. *Genes Chromosomes Cancer* 2006; **45**: 420–5.
40 Tagawa H, Tsuzuki S, Suzuki R *et al.* Genome-wide array-based comparative genomic hybridization of diffuse large B-cell lymphoma: comparison between CD5-positive and CD5-negative cases. *Cancer Res* 2004; **64**: 5948–55.
41 Pfaffl MW, Horgan GW, Dempfle L. Relative expression software tool (REST) for group-wise comparison and statistical analysis of relative expression results in real-time PCR. *Nucleic Acids Res* 2002; **30**: e36.
42 Heintz NH, Janssen YM, Mossman BT. Persistent induction of *c-fos* and *c-jun* expression by asbestos. *Proc Natl Acad Sci USA* 1993; **90**: 3299–303.
43 Shivapurkar N, Virmani AK, Wistuba II *et al.* Deletions of chromosome 4 at multiple sites are frequent in malignant mesothelioma and small cell lung carcinoma. *Clin Cancer Res* 1999; **5**: 17–23.
44 Bjorkqvist AM, Wolf M, Nordling S *et al.* Deletions at 14q in malignant mesothelioma detected by microsatellite marker analysis. *Br J Cancer* 1999; **81**: 1111–5.
45 Sandhu H, Dehnen W, Roller M, Abel J, Unfried K. mRNA expression patterns in different stages of asbestos-induced carcinogenesis in rats. *Carcinogenesis* 2000; **21**: 1023–9.
46 Knuuttila A, Jee KJ, Taskinen E, Wolff H, Knuutila S, Anttila S. Spindle cell tumours of the pleura: a clinical, histological and comparative genomic hybridization analysis of 14 cases. *Virchows Arch* 2006; **448**: 135–41.
47 Angel P, Karin M. The role of Jun, Fos and the AP-1 complex in cell proliferation and transformation. *Biochim Biophys Acta* 1991; **1072**: 129–57.
48 Lin DW, Coleman IM, Hawley S *et al.* Influence of surgical manipulation on prostate gene expression: implications for molecular correlates of treatment effects and disease prognosis. *J Clin Oncol* 2006; **24**: 3763–70.
49 Klabatsa A, Sheaff MT, Steele JP, Evans MT, Rudd RM, Fennell DA. Expression and prognostic significance of hypoxia-inducible factor 1α (HIF-1α) in malignant pleural mesothelioma (MPM). *Lung Cancer* 2006; **51**: 53–9.
50 Omasa T. Gene amplification and its application in cell and tissue engineering. *J Biosci Bioeng* 2002; **94**: 600–5.
51 Sasaki S, Kitagawa Y, Sekido Y *et al.* Molecular processes of chromosome 9p21 deletions in human cancers. *Oncogene* 2003; **22**: 3792–8.
52 Florl AR, Schulz WA. Peculiar structure and location of 9p21 homozygous deletion breakpoints in human cancer cells. *Genes Chromosomes Cancer* 2003; **23**: 141–8.
53 Raschke S, Balz V, Efferth T, Schulz WA, Florl AR. Homozygous deletions of CDKN2A caused by alternative mechanisms in various human cancer cell lines. *Genes Chromosomes Cancer* 2005; **42**: 58–67.
54 Suzuki M, Toyooka S, Shivapurkar N *et al.* Aberrant methylation profile of human malignant mesotheliomas and its relationship to SV40 infection. *Oncogene* 2005; **24**: 1302–8.
55 Shigemitsu K, Sekido Y, Usami N *et al.* Genetic alteration of the β-catenin gene (CTNNB1) in human lung cancer and malignant mesothelioma and identification of a new 3p21.3 homozygous deletion. *Oncogene* 2001; **20**: 4249–57.
56 Usami N, Sekido Y, Maeda O *et al.* Beta-catenin inhibits cell growth of a malignant mesothelioma cell line, NCI-H28, with a 3p21.3 homozygous deletion. *Oncogene* 2003; **22**: 7923–30.

doi: 10.1111/j.1349-7006.2006.00386.x

Carcinogenesis vol.28 no.8 pp.1718–1725, 2007
doi:10.1093/carcin/bgm104
Advance Access publication April 29, 2007

Impact of one-carbon metabolism-related gene polymorphisms on risk of lung cancer in Japan: a case–control study

Takeshi Suzuki[1,2], Keitaro Matsuo[1,6,*], Akio Hiraki[1], Toshiko Saito[1], Shigeki Sato[2], Yasushi Yatabe[3], Tetsuya Mitsudomi[4], Toyoaki Hida[5], Ryuzo Ueda[2] and Kazuo Tajima[1,6]

[1]Division of Epidemiology and Prevention, Aichi Cancer Center Research Institute, 1-1 Kanokoden, Chikusa-ku, Nagoya 464-8681, Japan, [2]Department of Internal Medicine and Molecular Science, Nagoya City University Graduate School of Medical Science, 1 Kawasumi, Mizuho-cho, Mizuho-ku, Nagoya 467-8601, Japan, [3]Department of Pathology and Molecular Diagnostics, [4]Department of Thoracic Surgery and [5]Department of Thoracic Oncology, Aichi Cancer Center Hospital, 1-1 Kanokoden, Chikusa-ku, Nagoya 464-8681, Japan and [6]Department of Epidemiology, Nagoya University Graduate School of Medicine, 65 Tsuruma-cho, Showa-ku, Nagoya 466-8550, Japan

*To whom correspondence should be addressed. Tel: +81 52 762 6111; Fax: +81 52 763 5233;
Email: kmatsuo@aichi-cc.jp

There is substantial evidence that the decreased risk of lung cancer with high intake of vegetables and fruits is linked to folate as a specific nutrient. Functional polymorphisms in genes encoding one-carbon metabolism enzymes, methylenetetrahydrofolate reductase (*MTHFR* C677T and A1298C), methionine synthase (*MTR* A2756G), methionine synthase reductase (*MTRR* A66G) and thymidylate synthase, influence folate metabolism and thus might be suspected of impacting on lung cancer risk. We therefore conducted a case–control study with 515 lung cancer cases newly and histologically diagnosed and 1030 age- and sex-matched non-cancer controls to clarify associations with these five polymorphisms according to lung cancer subtype. Gene–environment interactions with smoking and drinking habit and folate consumption were also evaluated by logistic regression analysis. None of the polymorphisms showed any significant impact on lung cancer overall risk by genotype alone, but on histology-based analysis increase in *MTHFR* 677T and 1298C alleles was associated with reduced risk of squamous/small cell carcinoma ($P = 0.029$), especially among heavy smokers ($P = 0.035$), whereas the *MTHFR* 677TT genotype was linked to decreased risk for these subtypes among heavy drinkers (odds ratio = 0.17, 95% confidence interval: 0.03–0.98). In addition, we found interactions between the *MTRR* A66G polymorphism and smoking ($P = 0.015$) and the *MTHFR* A1298C polymorphism and alcohol consumption ($P = 0.025$) for risk of lung cancer overall. In conclusion, the results suggest that *MTHFR* polymorphisms contribute to risk of squamous/small cell carcinomas of the lung, along with possible interactions among folate metabolism-related polymorphisms and smoking/drinking habits. Further evaluation is warranted.

Introduction

Lung cancer, with its four major histological types (adenocarcinoma, squamous cell carcinoma, large cell carcinoma and small cell carcinoma), currently claims >55 000 lives annually in Japan and has become the leading cause of cancer death (1). Despite rapid advances in treatment over recent decades, the prognosis has not greatly improved. Therefore, efforts toward primary prevention in addition to early detection have come under the spotlight.

Abbreviations: CI, confidence interval; FFQ, food frequency questionnaire; 5,10-methylene THF, 5,10-methylenetetrahydrofolate; MTHFR, methylenetetrahydrofolate reductase; MTR, methionine synthase; MTRR, methionine synthase reductase; OR, odds ratio; PCR, polymerase chain reaction; 2R, two repeat; TS, thymidylate synthase; VNTR, variable number of tandem repeat.

Many epidemiological studies have provided evidence that high consumption of vegetables and fruits is associated with a reduced risk of lung cancer (2–4). Folate is one of the constituents found in vegetables and fruits, and dietary folate may be one of the micronutrients that provide protection against lung carcinogenesis (5–7).

Biological functions of folate within so-called 'one-carbon metabolism' are to facilitate *de novo* deoxynucleoside triphosphate synthesis and to provide methyl groups required for intracellular methylation reactions. Folate deficiency is thought to increase the risk of cancer through impaired DNA repair synthesis and disruption of DNA methylation that may lead to proto-oncogene activation (8–10).

Methylenetetrahydrofolate reductase (MTHFR), methionine synthase (MTR), methionine synthase reductase (MTRR) and thymidylate synthase (TS) play important and interrelated roles in folate metabolism (Figure 1). The MTHFR reduces 5,10-methylenetetrahydrofolate (5,10-methylene THF) to 5-methyl THF, the primary circulating form of folate (11). The TS catalyzes the conversion of deoxyuridine monophosphate to deoxythymidine monophosphate using 5,10-methylene THF (12). The MTHFR product, 5-methyl THF, is the methyl group donor for the remethylation of homocysteine to methionine catalyzed by MTR (13). MTR activity is maintained by MTRR (14). Polymorphisms in the genes for *MTHFR* C677T and A1298C, *MTR* A2756G, *MTRR* A66G and *TS* 28 bp variable number of tandem repeat (VNTR) in the promoter region are known to have functional relevance (15). Thus, they might play roles in the etiology of lung cancer in combination with environmental factors such as folate consumption. Since information for this area of lung cancer is limited (16–22), we conducted the present case–control study, taking tobacco smoking, alcohol drinking and intake of folate into consideration.

Materials and methods

Subjects

The cases were 515 patients who were newly and histologically diagnosed as having lung cancer and not having any earlier history of cancer. Controls ($n = 1030$) were randomly selected and matched by age (±3 years) and sex to cases with a 1:2 case–control ratio from among the 2395 cancer-free individuals. All the subjects were recruited in the framework of the Hospital-based Epidemiologic Research Program at Aichi Cancer Center, as described elsewhere (23,24). In brief, information on lifestyle factors was collected using a self-administered questionnaire, checked by a trained interviewer, from all first-visit out-patients at Aichi Cancer Center Hospital aged 18–79 who were enrolled in Hospital-based Epidemiologic Research Program at Aichi Cancer Center between January 2001 and November 2005. Out-patients were also asked to provide blood samples. Each patient was asked about his or her lifestyle when healthy or before the current symptoms developed. Approximately 95% of eligible subjects complete the questionnaire and 60% provide blood samples. The data were loaded into a Hospital-based Epidemiologic Research Program at Aichi Cancer Center database and routinely linked with the hospital-based cancer registry system to update the data on cancer incidence. All participants gave written informed consent and the study was approved by Institutional Ethical Committee of Aichi Cancer Center.

Genotyping of MTHFR, MTR, MTRR and TS

DNA from each subject was extracted from the buffy coat fraction using BioRobot EZ1 and an EZ1 DNA Blood 350 ml Kit (Qiagen, Tokyo, Japan). The genotyping method was described in our previous reports with the polymerase chain reaction (PCR) TaqMan method using the GeneAmp PCR System 9700 or the 7500 Fast Real-Time PCR system (Applied Biosystems, Foster City, CA). Briefly, for the *MTHFR* C677T (dbSNP ID: rs677) and A1298C (rs1801131), as well as *MTR* A2756G (rs1805087) and *MTRR* A66G (rs1801394) polymorphisms, extracted DNA was amplified with validated probes (assay IDs: C__11975651_10, C__850486_20, C__12005959_10 and C__3068176_10, respectively; Applied Biosystems). The *TS* VNTR polymorphism was defined by PCR using 5′-CGTGGCTCCTGCGTTTCC-3′ and 5′-GAGCCGGCCACAGGCAT-3′ primers. In our laboratory, quality of genotyping is routinely assessed statistically using the Hardy–Weinberg test.

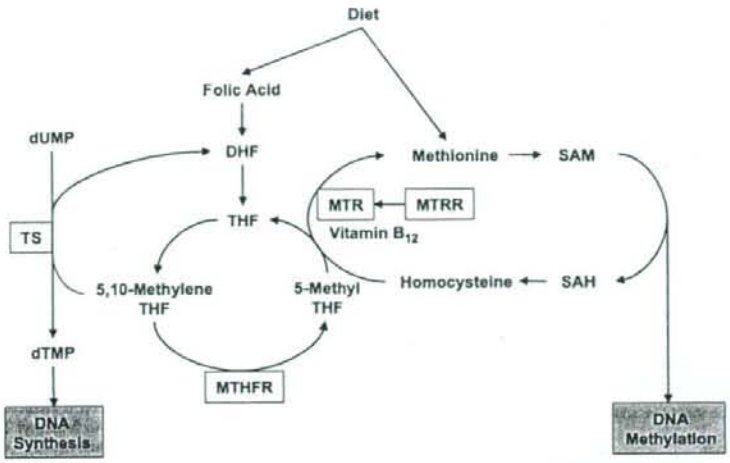

Fig. 1. Overview of folate metabolism. Enzymes with polymorphisms investigated in this study are boxed. THF, tetrahydrofolate; DHF, dihydrofolate; dUMP, deoxyuridine monophosphate; dTMP, deoxythymidine monophosphate; SAM, *S*-adenosylmethionine and SAH, *S*-adenosylhomocysteine.

When allelic distributions for controls depart from the Hardy–Weinberg frequency, genotyping is assessed using another method.

Intake assessment for folate and other nutrients

The consumption of folate and other nutrients was determined using a food frequency questionnaire (FFQ), described in detail elsewhere (25,26). Briefly, the FFQ consisted of 47 single food items with frequencies in the eight categories. We estimated the average daily intake of nutrients by multiplying the food intake (in grams) or serving size by the nutrient content per 100 g of food as listed in standard tables of food composition. Consumption of folate and other vitamins from supplements was not considered in total consumption because the questionnaire for multivitamins was not quantitative. Energy-adjusted intake of nutrients was calculated by the residual method (27). The FFQ was validated by referring to a 3-day weighed dietary record as a standard, which showed reproducibility and validity to be acceptable (28). The deattenuated correlation coefficients for energy-adjusted intakes of folate were 0.36 in men and 0.38 in women.

Consumption of tobacco and alcohol

Cumulative smoking dose was evaluated as pack-years, the product of the number of packs consumed per day and years of smoking. Smoking habit was entered for four categories of never, former and current smokers of <40 and ≥40 pack-years. Former smokers were defined as those who quit smoking at least 1 year before the survey. Consumption of each type of beverage (Japanese sake, beer, shochu, whiskey and wine) was determined by the average number of drinks per day, which was then converted into a Japanese sake (rice wine) equivalent. One drink equates to one 'go' (180 ml) of Japanese sake, which contains 23 g of ethanol, equivalent to one large bottle (633 ml) of beer, two shots (60 ml) of whiskey and two and a half glasses of wine (200 ml). One drink of 'shochu' (distilled spirit), which contains 25% ethanol, was rated as 108 ml. Total amount of alcohol consumption was estimated as the summarized amount of pure alcohol consumption (gram per drink) of Japanese sake, beer, shochu, whiskey and wine among current regular drinkers. Drinking habit was entered for four categories of never, former, current moderate and heavy drinkers. Heavy drinkers were defined as those currently drinking alcoholic beverages 5 days or more per week in a daily amount of 46 g (two Japanese drinks) or more, whereas moderate drinkers were defined as those currently consuming less frequently than 5 days/week, in lower amounts, or both. Former drinkers were defined as those who quit drinking at least 1 year before the survey. Former or current smokers and drinkers were categorized as 'smokers' and 'drinkers', respectively.

Statistical analysis

To assess the strength of the associations between polymorphic genes involved in folate metabolism and risk of lung cancer, odds ratio (ORs) with 95% confidence intervals (CIs) were estimated using age- and sex-matched conditional logistic models adjusted for potential confounders. For stratified and interaction analysis by smoking and drinking habit and folate intake, an unconditional logistic regression model was used because the matching was not retained after stratification by smoking and drinking habit and folate intake. Folate and other nutrient intakes were categorized into three groups as: first, second and third tertiles of dietary intake among controls. Potential confounders considered in the multivariate analyses were age, sex, smoking habit (never smokers, former smokers, current smokers of <40 or ≥40 pack-years), drinking habit (never drinkers, former drinkers, moderate drinkers or heavy drinkers), body mass index (<18.5, 18.5–24.9 or ≥25.0), total energy intake (as a continuous variable), dietary carotene intake (μg/day, tertiles), dietary vitamin C intake (mg/day, tertiles), dietary vitamin E intake (mg/day, tertiles), dietary folate intake (μg/day, tertiles), multivitamin use (at least once per week for 1 year or longer: yes or no) and referral pattern (patient's discretion, family recommendation, referral from other clinics, secondary screening after primary screening or others). Missing values for each covariate were treated as an additional category in the variable and were included in the logistic model.

For the histology-based analysis, we combined squamous cell carcinoma and small cell carcinoma, because tumors of these subtypes were small in number and both are consistently more related with smoking as compared with adenocarcinomas. Considering potential effects of two polymorphisms (*MTHFR* C677T and *MTHFR* A1298C) on lung risk, we evaluated associations with their combined genotypes. Trend of genotype was assessed by score test applying score for each genotype (0, homozygous for reference allele or combined reference genotypes; 1, heterozygote or one reference genotype and 2, homozygous non-reference allele or non-reference genotype).

Gene–environment interactions between smoking and drinking habit and folate intake and genotypes in each polymorphism were evaluated under the multiplicative assumption. Products of scores for genotype (0, homozygous; 1, heterozygote and 2, homozygous or 0, referent alleles and 1, non-referent alleles) and smoking habit (0, non-smoker and 1, smoker), drinking habit (0, non-drinker and 1, drinker), folate intake (0, tertile 1 and 1, tertile 2 + 3) or combined smoking–drinking habit (0, non-smoker and non-drinker; 1, smoker and non-drinker or drinker and non-smoker and 2, smoker/drinker) were included as interaction terms. Differences in categorized demographic variables between the cases and controls were tested by the Chi-squared test. Mean values for age and total energy intake were compared for cases and controls by the Student's *t*-test. Accordance with the Hardy–Weinberg equilibrium was checked for controls using the Chi-squared test and the exact *P*-value was used to assess any discrepancies between genotypes and allele frequencies. A *P*-value <0.05 was considered statistically significant. All analyses were performed using STATA version 9 (Stata Corp., College Station, TX).

Results

Data from 515 lung cancer cases, comprising 316 (61.4%) adenocarcinomas, 91 (17.7%) squamous cell carcinomas, 55 (10.7%) small

cell carcinomas, 40 (7.8%) large cell carcinomas and 13 (2.5%) others, and 1030 controls were available for analysis. Table I shows the distribution of cases and controls by background characteristics. Age and sex were appropriately matched. Smoking habits differed to a large extent between cases and controls. The proportion of 40 pack-years or more current smokers in cases was significantly higher than controls. Heavy drinkers in the cases were significantly higher than for the controls. Among cases, the proportion of lower body mass index was higher, consistent with previous study (29). Total energy intake did not differ between cases and controls. Significant lower intake of dietary carotene was found among the cases. For other nutrients lower proportions of the highest intake group among the cases also were found, including for folate, but these were not statistically significant. With regard to referral pattern, referral from other clinics was frequent, whereas patient discretion and secondary screening after primary screening were less common among the case group than the control group.

Table II shows genotype distributions for *MTHFR*, *MTR*, *MTRR* and *TS* and their ORs and 95% CIs for lung cancer risk according to histological subtypes. The genotype frequencies for all the polymorphisms were in accordance with the Hardy–Weinberg law in controls: *MTHFR* C677T ($P = 0.17$), *MTHFR* A1298C ($P = 0.51$), *MTR* A2756G ($P = 0.17$), *MTRR* A66G ($P = 0.85$) and *TS* VNTR ($P = 0.51$). On analysis of lung cancer overall, a slightly reduced risk was observed with the *MTHFR* 677TT genotype, but without statistical significance. The genotype frequencies for *TS* VNTR were quite varied; however, two repeat (2R) and three repeat alleles were dominant. The 2R/2R genotype showed decreased risk of lung cancer as compared with the non-2R homozygous, although again this was not significant. On subanalysis according to histological subtypes, the combination of *MTHFR* C677T and A1298C polymorphisms showed a significant decreased risk of squamous/small cell carcinoma among individuals with two or more *MTHFR* 677T and/or 1298C alleles (OR = 0.34, 95% CI: 0.13–0.92, trend $P = 0.029$), compared with those with *MTHFR* 677CC and 1298AA genotypes. In contrast, none of the polymorphisms showed any significant impact on adenocarcinoma risk.

To further evaluate the impact of *MTHFR* polymorphisms with regard to squamous/small cell carcinoma, we conducted stratified analysis by smoking and drinking habit (Table III). Among heavy drinkers, the *MTHFR* 677TT genotype conferred a significant decreased risk (OR = 0.17, 95% CI: 0.03–0.98, trend $P = 0.041$). A significant decreased risk among 40 pack-years or more current smokers was observed as number of *MTHFR* 677T or 1298C alleles increased (trend $P = 0.035$). No clear association was found for lung cancers overall or for adenocarcinomas in the stratified analysis (data not shown).

Table IV shows data for the combinations of gene and environmental factors with reference to lung cancer overall risk. The interaction with smoking was significant for the *MTRR* A66G genotype ($P = 0.015$). Among non-smokers, risk was reduced with increase in the number of *MTRR* G alleles, whereas a trend for increased risk was observed among smokers. A significant interaction between drinking habits and the *MTHFR* A1298C genotype was found ($P = 0.025$). These two interactions were especially noteworthy for adenocarcinomas when histology-based analyses were conducted (data not shown). We were not able to analyze the smoking interaction for squamous/small cell due to insufficient number of non-smokers in this category. No obvious interaction was found between folate intake and the polymorphisms.

Considering the possible effects of both tobacco smoking and alcohol drinking on folate, we further examined the impact of four-way combinations of these two factors, folate intake and the polymorphisms on lung cancer risk (Table V). The *MTRR* A66G genotype showed a significant interaction among the subjects with tertiles 2 or 3 of folate intake ($P = 0.023$). The risk with the *MTRR* 66GG was consistently decreased among non-smoker/non-drinker subjects with adequate folate intake (OR = 0.20, 95% CI: 0.04–0.91).

Table I. Characteristics of cases and controls

	Cases ($n = 515$), n(%)	Controls ($n = 1030$), n(%)	P-value
Age			
<50	53 (10.3)	108 (10.5)	
50–59	142 (27.6)	283 (27.5)	
60–69	193 (37.5)	389 (37.8)	
70–79	127 (24.7)	250 (24.3)	1.00
Mean age ± SD	61.9 ± 9.9	61.8 ± 9.8	0.87
Sex			
Male	381 (74.0)	762 (74.0)	
Female	134 (26.0)	268 (26.0)	1.00
Smoking status			
Never	129 (25.0)	401 (38.9)	
Former[a]	111 (21.6)	310 (30.1)	
Current (pack-years)			
0–39	71 (13.8)	149 (14.5)	
≥40	197 (38.3)	161 (15.6)	<0.01
Unknown	7 (1.4)	9 (0.9)	
Drinking status			
Never	196 (38.1)	378 (36.7)	
Former[a]	15 (2.9)	56 (5.4)	
Current			
Moderate[b]	192 (37.3)	454 (44.1)	
Heavy[c]	98 (19.0)	119 (11.6)	<0.01
Unknown	14 (2.7)	23 (2.2)	
BMI			
<18.5	38 (7.4)	55 (5.3)	
18.5–24.9	381 (74.0)	720 (69.9)	
≥25.0	94 (18.3)	249 (24.2)	0.03
Unknown	2 (0.4)	6 (0.6)	
Mean total energy ± SD, kcal/day	1670 ± 372	1677 ± 352	0.73
Carotene (μg/day)			
Tertile 1 (1331.2–2305.9)	200 (38.8)	341 (33.1)	
Tertile 2 (2306.0–3312.6)	149 (28.9)	341 (33.1)	
Tertile 3 (3312.7–12801.4)	158 (30.7)	341 (33.1)	0.04
Unknown	8 (1.6)	7 (0.7)	
Vitamin C (mg/day)			
Tertile 1 (26.8–74.5)	188 (36.5)	342 (33.2)	
Tertile 2 (74.6–102.0)	161 (31.3)	342 (33.2)	
Tertile 3 (102.1–364.5)	159 (30.7)	341 (33.1)	0.15
Unknown	7 (1.4)	5 (0.5)	
Vitamin E (total α-mg/day)			
Tertile 1 (1.5–4.8)	193 (37.5)	342 (33.2)	
Tertile 2 (4.9–6.3)	168 (32.6)	342 (33.2)	
Tertile 3 (6.4–17.1)	151 (29.3)	342 (33.2)	0.29
Unknown	3 (0.6)	4 (0.4)	
Folate intake (μg/day)			
Tertile 1 (139.5–274.5)	191 (37.1)	342 (33.2)	
Tertile 2 (274.6–354.9)	156 (30.3)	342 (33.2)	
Tertile 3 (355.0–1481.0)	162 (31.5)	341 (33.1)	0.18
Unknown	6 (1.2)	5 (0.5)	
Multivitamin use (at least once per week for 1 year or longer)			
Yes	111 (21.6)	253 (24.6)	
No	380 (73.8)	721 (70.0)	0.30
Unknown	24 (4.7)	56 (5.4)	
Referral pattern to our hospital			
Patient's discretion	52 (10.1)	306 (29.7)	
Family recommendation	86 (16.7)	195 (18.9)	
Referral from other clinics	287 (55.7)	300 (29.1)	
Secondary screening after primary screening	83 (16.1)	214 (20.8)	
Others	2 (0.4)	10 (1.0)	<0.01
Unknown	5 (1.0)	5 (0.5)	

SD: standard deviation, BMI: body mass index.
[a]Former smokers and drinkers were defined as subjects who had quit smoking and drinking at least 1 year previously.
[b]Moderate drinker means <46 g ethanol/drink and/or <5 days/week.
[c]Heavy drinker means ≥46 g ethanol/drink and ≥5 days/week.

Table II. *MTHFR, MTR, MTRR* and *TS* genotype distributions, and ORs for lung cancer according to histology

	All			Adenocarcinoma			Squamous + small cell carcinoma		
	Cases (n = 515), n (%)	Controls (n = 1030), n (%)	ORs[a] (95% CIs)	Cases (n = 316), n (%)	Controls (n = 632), n (%)	ORs[a] (95% CIs)	Cases (n = 146), n (%)	Controls (n = 292), n (%)	ORs[a] (95% CIs)
MTHFR (C677T)									
CC	182 (35.3)	379 (36.8)	1.00 (ref.)	109 (34.5)	237 (37.5)	1.00 (ref.)	54 (37.0)	103 (35.3)	1.00 (ref.)
CT	256 (49.7)	474 (46.0)	1.05 (0.81–1.37)	158 (50.0)	288 (45.6)	1.01 (0.72–1.41)	72 (49.3)	134 (45.9)	0.83 (0.43–1.58)
TT	77 (15.0)	177 (17.2)	0.75 (0.52–1.09)	49 (15.5)	107 (16.9)	0.85 (0.53–1.34)	20 (13.7)	55 (18.8)	0.44 (0.16–1.18)
P_{trend}[b]			0.260			0.567			0.129
MTHFR (A1298C)									
AA	341 (66.2)	652 (63.3)	1.00 (ref.)	210 (66.5)	416 (65.8)	1.00 (ref.)	94 (64.4)	175 (59.9)	1.00 (ref.)
AC	149 (28.9)	322 (31.3)	0.85 (0.65–1.13)	90 (28.5)	189 (29.9)	0.94 (0.67–1.33)	46 (31.5)	99 (33.9)	0.84 (0.42–1.68)
CC	22 (4.3)	45 (4.4)	1.01 (0.56–1.83)	14 (4.4)	22 (3.5)	1.46 (0.68–3.16)	5 (3.4)	14 (4.8)	0.40 (0.07–2.28)
UK[c]	3 (0.6)	11 (1.1)		2 (0.6)	5 (0.8)		1 (0.7)	4 (1.4)	
P_{trend}[b]			0.428			0.822			0.348
MTHFR C677T and A1298C combined									
Number of Variants									
0	76 (14.8)	174 (16.9)	1.00 (ref.)	43 (13.6)	118 (18.7)	1.00 (ref.)	23 (15.8)	41 (14.0)	1.00 (ref.)
1	273 (53.0)	471 (45.7)	1.19 (0.83–1.71)	171 (54.1)	293 (46.4)	1.46 (0.93–2.27)	76 (52.1)	130 (44.5)	0.52 (0.19–1.40)
≦2	163 (31.7)	374 (36.3)	0.84 (0.58–1.24)	100 (31.6)	216 (34.2)	1.10 (0.68–1.77)	46 (31.5)	117 (40.1)	0.34 (0.13–0.92)
UK[c]	3 (0.6)	11 (1.1)		2 (0.6)	5 (0.8)		1 (0.7)	4 (1.4)	
P_{trend}[b]			0.110			0.819			0.029
MTR (A2756G)									
AA	319 (61.9)	698 (67.8)	1.00 (ref.)	192 (60.8)	423 (66.9)	1.00 (ref.)	100 (68.5)	195 (66.8)	1.00 (ref.)
AG	175 (34.0)	291 (28.3)	1.23 (0.94–1.60)	109 (34.5)	184 (29.1)	1.26 (0.91–1.75)	42 (28.8)	84 (28.8)	0.80 (0.42–1.52)
GG	21 (4.1)	40 (3.9)	1.04 (0.55–2.00)	15 (4.7)	25 (4.0)	1.35 (0.62–2.91)	4 (2.7)	13 (4.5)	0.49 (0.07–3.38)
UK[c]	0 (0)	1 (0.1)							
P_{trend}[b]			0.227			0.146			0.364
MTRR (A66G)									
AA	235 (45.6)	484 (47.0)	1.00 (ref.)	148 (46.8)	294 (46.5)	1.00 (ref.)	63 (43.2)	136 (46.6)	1.00 (ref.)
AG	226 (43.9)	446 (43.3)	1.02 (0.79–1.31)	139 (44.0)	275 (43.5)	0.93 (068–1.28)	64 (43.8)	131 (44.9)	1.18 (0.60–2.31)
GG	54 (10.5)	100 (9.7)	0.96 (0.62–1.47)	29 (9.2)	63 (10.0)	0.91 (0.52–1.58)	19 (13.0)	25 (8.6)	1.11 (0.38–3.21)
P_{trend}[b]			0.939			0.638			0.718
TS VNTR									
Non-2R/non-2R	372 (72.2)	721 (70.0)	1.00 (ref.)	236 (74.7)	434 (68.7)	1.00 (ref.)	101 (69.2)	212 (72.6)	1.00 (ref.)
2R/non-2R	132 (25.6)	278 (27.0)	0.96 (0.73–1.27)	73 (23.1)	181 (28.6)	0.81 (0.57–1.13)	43 (29.5)	69 (23.6)	1.26 (0.61–2.59)
2R/2R	10 (1.9)	31 (3.0)	0.63 (0.29–1.39)	6 (1.9)	17 (2.7)	0.62 (0.22–1.73)	2 (1.4)	11 (3.8)	0.23 (0.03–1.62)
UK[c]	1 (0.2)	0 (0)		1 (0.3)	0 (0)				
P_{trend}[b]			0.394			0.137			0.653

[a]ORs were matched for age and sex and adjusted for smoking habit, drinking habit, body mass index, total energy intake, carotene intake, vitamin C intake, vitamin E intake, multivitamin use and referral pattern to our hospital.

[b]Trend of genotype was assessed by score test applying score for each genotypes (0, homozygous for reference allele or combined reference genotypes; 1, heterozygote or one reference genotype and 2, homozygous non-reference allele or non-reference genotype).

[c]UK denotes genotype unknown.

Table III. Stratification analysis by smoking and drinking habit for the *MTHFR* polymorphisms in squamous/small cell carcinoma

	Smoking status						Drinking status							
	Smokers		0–39 pack-years		40 ≥ pack-years		Non-drinkers		Drinkers		Moderate drinkers		Heavy drinkers	
	Cases/ controls	ORs[a] (95% CIs)	Cases/ controls	ORs[a] (95% CIs)	Cases/ controls	ORs[a] (95% CIs)	Cases/ controls	ORs[a] (95% CIs)	Cases/ controls	ORs[a] (95% CIs)	Cases/ controls	ORs[a] (95% CIs)	Cases/ controls	ORs[a] (95% CIs)
MTHFR (C677T)														
CC	53/229	1.00 (ref.)	7/65	1.00 (ref.)	35/58	1.00 (ref.)	15/143	1.00 (ref.)	39/236	1.00 (ref.)	22/168	1.00 (ref.)	14/38	1.00 (ref.)
CT	72/293	0.94 (0.61–1.45)	10/65	1.83 (0.40–8.47)	41/73	0.85 (0.43–1.67)	23/176	0.89 (0.36–2.21)	49/298	1.08 (0.63–1.84)	26/206	1.02 (0.48–2.16)	14/61	0.37 (0.09–1.63)
TT	20/107	0.81 (0.44–1.51)	4/19	5.63 (0.60–53.25)	11/30	0.50 (0.20–1.29)	3/59	0.52 (0.09–3.00)	17/118	0.90 (0.44–1.84)	8/80	0.85 (0.30–2.43)	5/20	0.17 (0.03–0.98)
P_{trend}[b]		0.528		0.151		0.179		0.519		0.871		0.817		0.041
MTHFR (A1298C)														
AA	93/406	1.00 (ref.)	15/106	1.00 (ref.)	57/97	1.00 (ref.)	29/232	1.00 (ref.)	65/420	1.00 (ref.)	36/293	1.00 (ref.)	18/74	1.00 (ref.)
AC	46/186	1.04 (0.68–1.61)	5/33	0.84 (0.15–4.63)	26/55	0.68 (0.35–1.33)	11/123	0.67 (0.26–1.77)	35/199	1.17 (0.69–2.01)	18/139	0.99 (0.46–2.11)	13/40	3.61 (0.87–14.96)
CC	5/30	0.80 (0.28–2.26)	0/8	NA[d]	4/9	0.84 (0.21–3.31)	1/20	0.30 (0.02–3.82)	4/25	1.05 (0.31–3.51)	2/17	1.03 (0.19–5.74)	2/5	1.05 (0.08–13.61)
UK[c]	1/7		1/2				0/3		1/8		0/5			
P_{trend}[b]		0.916		0.381		0.362		0.263		0.649		0.998		0.300
MTHFR C677T and A1298C combined														
Number of Variants														
0	22/105	1.00 (ref.)	3/37	1.00 (ref.)	15/22	1.00 (ref.)	6/64	1.00 (ref.)	17/110	1.00 (ref.)	13/81	1.00 (ref.)	4/15	1.00 (ref.)
1	76/295	1.08 (0.61–1.92)	11/72	0.63 (0.10–3.98)	47/73	0.97 (0.39–2.43)	28/169	1.02 (0.30–3.50)	48/302	1.13 (0.57–2.27)	22/211	0.57 (0.23–1.44)	17/58	0.93 (0.12–6.96)
≦2	46/222	0.88 (0.48–1.63)	6/38	2.40 (0.30–18.97)	25/66	0.44 (0.17–1.17)	7/142	036 (0.08–1.56)	39/232	1.15 (0.56–2.36)	21/157	0.82 (0.32–2.13)	12/46	0.30 (0.04–2.55)
UK[c]	1/7		1/2				0/3		1/8		0/5			
P_{trend}[b]		0.557		0.397		0.035		0.109		0.751		0.860		0.148

Data were not available in non-smokers because of absence of subjects in this category.

[a]ORs were adjusted for age, sex, smoking habit, drinking habit, body mass index, total energy intake, carotene intake, vitamin C intake, vitamin E intake, folate intake, multivitamin use and referral pattern to our hospital.

[b]Trend of genotype was assessed by score test applying score for each genotypes (0, homozygous for reference allele; 1, heterozygote and 2, homozygous non-reference allele).

[c]UK denotes genotype unknown.

[d]NA indicates not available because of absence of subjects in this category.

Table IV. Interaction between *MTHFR*, *MTR*, *MTRR* and *TS* polymorphisms and smoking and drinking habit and folate intake for lung cancer risk

	Smoking habit			Drinking habit			Folate intake		
	Non-smoker	Smoker	*P* interaction[b]	Non-drinker	Drinker	*P* interaction[b]	Tertile 1 (139.5–274.5 μg/day)	Tertile 2 + 3 (274.6–1481.0 μg/day)	*P* interaction[b]
	ORs[a] (95% CIs)	ORs[a] (95% CIs)		ORs[a] (95% CIs)	ORs[a] (95% CIs)		ORs[a] (95% CIs)	ORs[a] (95% CIs)	
MTHFR (C677T)									
CC	1.00 (ref.)	2.59 (1.61–4.17)		1.00 (ref.)	1.02 (0.67–1.55)		1.00 (ref.)	0.82 (1.34–0.82)	
CT	1.09 (0.69–1.73)	2.84 (1.79–4.52)		1.17 (0.77–1.78)	1.07 (0.72–1.60)		1.03 (1.58–1.03)	0.93 (1.50–0.93)	
TT	0.68 (0.36–1.29)	2.55 (1.48–4.40)	0.430	1.21 (0.68–2.14)	0.74 (0.45–1.23)	0.207	0.98 (1.82–0.98)	0.69 (1.22–0.69)	0.851
MTHFR (A1298C)									
AA	1.00 (ref.)	2.80 (1.88–4.18)		1.00 (ref.)	0.76 (0.56–1.04)		1.00 (ref.)	0.81 (1.24–0.81)	
AC	0.88 (0.55–1.39)	2.61 (1.67–4.07)		0.73 (0.48–1.12)	0.77 (0.53–1.11)		0.73 (1.14–0.73)	0.80 (1.27–0.80)	
CC	1.60 (0.61–4.19)	1.84 (0.85–3.96)	0.464	0.36 (0.12–1.04)	1.20 (0.58–2.47)	0.025	1.72 (4.44–1.72)	0.52 (1.18–0.52)	0.824
MTR (A2756G)									
AA	1.00 (ref.)	3.08 (2.07–4.57)		1.00 (ref.)	0.93 (0.68–1.28)		1.00 (ref.)	0.93 (1.40–0.93)	
AG	1.65 (1.05–2.59)	3.49 (2.26–5.40)		1.55 (1.03–2.33)	1.12 (0.77–1.61)		1.56 (2.40–1.56)	1.08 (1.70–1.08)	
GG	0.90 (0.27–2.94)	3.08 (1.45–6.53)	0.348	0.76 (0.27–2.14)	1.18 (0.54–2.56)	0.798	1.24 (3.45–1.24)	0.85 (1.92–0.85)	0.285
MTRR (A66G)									
AA	1.00 (ref.)	2.04 (1.31–3.16)		1.00 (ref.)	1.21 (0.83–1.76)		1.00 (ref.)	0.73 (1.15–0.73)	
AG	0.70 (0.45–1.09)	2.31 (1.49–3.58)		1.53 (1.02–2.27)	0.90 (0.61–1.32)		0.75 (1.14–0.75)	0.83 (1.31–0.83)	
GG	0.46 (0.20–1.09)	2.60 (1.49–4.56)	0.015	0.88 (0.45–1.73)	1.18 (0.67–2.06)	0.212	1.41 (2.82–1.41)	0.58 (1.09–0.58)	0.907
TS VNTR									
Non-2R/non-2R	1.00 (ref.)	2.62 (1.78–3.85)		1.00 (ref.)	0.93 (0.69–1.26)		1.00 (ref.)	0.88 (1.32–0.88)	
2R/non-2R	0.84 (0.51–1.37)	2.52 (1.64–3.88)		1.01 (0.65–1.55)	0.85 (0.58–1.24)		1.02 (1.60–1.02)	0.80 (1.28–0.80)	
2R/2R	0.60 (0.15–2.36)	1.70 (0.64–4.53)	0.668	0.82 (0.19–3.53)	0.44 (0.17–1.12)	0.550	0.66 (2.62–0.66)	0.48 (1.29–0.48)	0.673

[a]ORs were adjusted for age, sex, smoking habit, drinking habit, body mass index, total energy intake, carotene intake, vitamin C intake, vitamin E intake, folate intake, multivitamin use and referral pattern to our hospital.
[b]Interaction was modeled as a product of smoking habit (0, non-smoker and 1, smoker), drinking habit (0, non-drinker and 1, drinker), folate intake in score (0, tertile 1 and 1, textile 2 + 3) and genotype in score.

Discussion

The present study showed a significant impact of *MTHFR* C677T and *MTHFR* A1298C in combination for risk of the most smoking related subtypes of lung cancer, squamous and small cell carcinomas. Moreover, this effect was prominent among heavy smokers. The *MTHFR* 677TT genotype was inversely associated with squamous/small cell carcinoma risk among heavy drinkers. In combination analysis of smoking, drinking and folate consumption, several potential gene–environment interactions were suggested, between (i) the *MTRR* A66G polymorphism and smoking and (ii) the *MTHFR* A1298C polymorphism and alcohol consumption.

High dietary intake of folate has been found to decrease the risk of lung cancer in several epidemiological studies (5–7). Although our result for folate did not reach statistically significance, the observed trend was accordant with other studies. Two small-sized clinical trials found folate and vitamin B_{12} supplementation to reverse atypia among patients with bronchial squamous metaplasia, a precursor of squamous cell carcinoma of the lung (30,31). One might therefore hypothesize a protective effect of folate on lung cancer, but there are also epidemiological studies providing no support for this concept (32–35). Considering the fact that functional polymorphisms in folate-related genes may contribute to alteration of folate metabolism (15), it is biologically plausible to hypothesize that the polymorphisms or the gene–environment interactions rather than the folate intake alone have the impact on lung cancer risk.

Hitherto, only a few studies have investigated associations between one-carbon metabolism-related gene polymorphisms and lung cancer risk. The *MTHFR* 677TT genotype has been reported to decrease risk of lung cancer in female Caucasians (20), but the results were inconsistent in other case–control studies (17,19). The *MTHFR* 1298CC and *MTRR* 66AG or GG genotypes were associated with significantly increased risk (20,21), whereas *MTR* and *TS* enhancer region polymorphisms in the Caucasians studies demonstrated no link (21,22). Our results of overall analysis added evidence for a null association in this controversial issue. However, of note in this study was the fact that *MTHFR* 677T and/or *MTHFR* 1298C alleles were associated with reduced risk of squamous/small cell carcinomas, especially among heavy smokers and drinkers. It has been shown that subjects with the *MTHFR* 677TT and *MTHFR* 1298CC genotypes have a reduction in enzyme activity compared with the wild-type homozygous, 677CC and 1298AA genotypes (36–38). This would lead to high 5,10-methylene THF concentrations, which may provide more one-carbon groups for thymidylate synthesis, thereby enhancing DNA synthesis and repair ability. Thus, it is biologically reasonable that individuals harboring the *MTHFR* 677T and *MTHFR* 1298C alleles among heavy smokers and drinkers have lower risk of squamous/small cell carcinoma development, given that carcinogenesis is strongly related with the accumulation of DNA damage. To our knowledge, this is the first indication of protective effects of combinations of *MTHFR* polymorphisms for this histologic subtype. These data provide support for the hypothesis of links between one-carbon metabolism and tobacco and alcohol influence on squamous/small cell carcinoma carcinogenesis. Regarding other body sites, our previous study on esophagus cancers, which are almost all squamous cell carcinomas in Japan, demonstrated that the *MTHFR* 677TT had the protective effects among heavy drinkers, consistent with the present study (39).

One difficulty exists in distinguishing effects of smoking and drinking on lung cancer risk. In the present study, of 33 heavy drinkers in squamous/small cell carcinoma cases, 24 (72.7%) cases were heavy smokers, so we may not conclude an independent protective effect of *MTHFR* 677TT genotypes among heavy drinkers, although adjustment for smoking habits was performed. On the other hand, all cases with squamous/small cell carcinomas were smokers except one and 60% (85/142) in this subtype were heavy smokers (40 pack-years or more). Alcohol drinking as well as tobacco smoking is considered to induce DNA damage and resultant modification of nucleotides (40,41). In addition, high intake of alcohol can lead to folate depletion

Table V. Impact of combination of smoking and drinking habit by folate intake and the polymorphisms on lung cancer risk

	Folate intake							
	Tertile 1 (139.5–274.5 μg/day)				Tertile 2 + 3 (274.6–1481.0 μg/day)			
	Non-smoker/non-drinker	Smoker/non-drinker or non-smoker/drinker	Smoker/drinker[a]	*P* interaction[c]	Non-smoker/non-drinker	Smoker/non-drinker or non-smoker/drinker	Smoker/drinke[a]	*P* interaction[c]
	ORs[b] (95% CIs)	ORs[b] (95% CIs)	ORs[b] (95% CIs)		ORs[b] (95% CIs)	ORs[b] (95% CIs)	ORs[b] (95% CIs)	
MTHFR (C677T)								
CC	1.00 (ref.)	1.33 (0.44–3.99)	1.60 (0.58–4.41)		1.00 (ref.)	1.82 (0.90–3.67)	2.89 (1.43–5.84)	
CT + TT	0.61 (0.19–1.98)	1.66 (0.62–4.48)	1.55 (0.58–4.18)	0.763	1.54 (0.83–2.89)	1.48 (0.79–2.80)	2.93 (1.50–5.73)	0.389
MTHFR (A1298C)								
AA	1.00 (ref.)	3.18 (1.20–8.42)	2.78 (1.06–7.27)		1.00 (ref.)	0.97 (0.57–1.65)	1.70 (0.97–3.00)	
AC + CC	1.68 (0.52–5.48)	1.63 (0.55–4.81)	2.33 (0.84–6.47)	0.701	0.56 (0.29–1.08)	1.04 (0.56–1.91)	2.04 (1.10–3.76)	0.078
MTR (A2756G)								
AA	1.00 (ref.)	2.13 (0.90–5.04)	1.95 (0.83–4.62)		1.00 (ref.)	1.11 (0.64–1.92)	2.74 (1.53–4.89)	
AG + GG	1.63 (0.46–5.72)	3.00 (1.12–8.00)	3.28 (1.34–8.02)	0.826	1.38 (0.74–2.55)	2.03 (1.09–3.77)	2.16 (1.15–4.05)	0.069
MTRR (A66G)								
AA + AG	1.00 (ref.)	2.17 (1.00–4.73)	2.27 (1.05–4.91)		1.00 (ref.)	1.14 (0.71–1.82)	1.98 (1.18–3.32)	
GG	3.96 (0.49–32.23)	3.19 (1.02–10.03)	2.77 (0.88–8.78)	0.384	0.20 (0.04–0.91)	0.67 (0.24–1.88)	2.34 (1.12–4.90)	0.023
TS VNTR								
Non-2R/non-2R	1.00 (ref.)	1.75 (0.74–4.16)	2.14 (0.92–4.96)		1.00 (ref.)	0.95 (0.56–1.60)	2.04 (1.17–3.55)	
2R/non-2R + 2R/2R	0.87 (0.24–3.07)	2.38 (0.92–6.18)	1.48 (0.57–3.82)	0.367	0.58 (0.28–1.20)	1.30 (0.71–2.39)	1.65(0.90–3.05)	0.769

[a]Subjects who are both smoker and drinker.
[b]ORs were adjusted for age, sex, body mass index, total energy intake, carotene intake, vitamin C intake, vitamin E intake, multivitamin use and referral pattern to our hospital.
[c]Interaction was modeled as a product of smoking/drinking habit (0, non-smoker/non-drinker; 1, smoker/non-drinker or drinker/non-smoker and 2, smoker/drinker) and genotype in score.

(42). Therefore, it is within expectation that the *MTHFR* 677T allele, associated with high 5,10-methylene THF concentrations, may have the potential to protect against squamous/small cell carcinomas in tobacco consumers drinking large amounts of alcohol.

It was previously reported that lung cancer risk is higher with the *MTRR* 66AG/GG genotypes than the *MTRR* 66AA genotype among former smokers, but this did not extend to never and current smokers (21). Here, interaction between this gene and smoking habit was observed. Furthermore, the *MTRR* GG genotype exhibited a protective effect in low-risk subjects (non-smokers/non-drinkers with adequate folate intake). Several cytogenetic biomarker studies suggested that some polymorphisms involved in metabolic activation/deactivation or in DNA repair have been expected to be of special importance in modulating tobacco and alcohol carcinogen effects (43). A recent study reported a positive association with the modulating effect of the *MTRR* polymorphism on micronucleus frequency in peripheral blood lymphocytes, one of the cytogenetic markers (44), which is probably to increase by smoking (45) and drinking (46). The higher micronucleus frequency recorded in *MTRR* 66GG genotype with respect to AG or AA genotype is suggestive of a role of this polymorphism in modulation of chromosome stability, so that the findings may be consistent with our results. Further studies on the underlying mechanisms of the *MTRR* polymorphism thus appear warranted.

We found an interaction between the drinking habit and *MTHFR* A1298C polymorphisms for lung cancer risk, with decreased risk among non-drinkers. A Caucasian study showed that the *MTHFR* 1298CC genotype elevated risk among both drinkers and non-drinkers but only in women (20). The *MTHFR* A1298C is associated with decreased enzymatic activity (37,38) and would be expected to exert a similar effect to *MTHFR* C677T, with mutant alleles more protective among drinkers (27,39). There is no clear biological explanation for our results, and we cannot rule out the possibility that our observations for *MTHFR* A1298C were due to chance. Replication in a future study is needed.

Several potential limitations of the present study warrant consideration. First, internal validity of this hospital-based study is a potential threat to causal inference. We used non-cancer patients at our hospital as controls, given the likelihood that our cases arose within this population base, but individuals selected randomly from our control population were earlier shown to be similar to the general population in terms of the exposure of interest (47). Equivalence in the genotype distribution for the *MTHFR* C677T polymorphism between our controls and the general population has also been reported (48). To account for variation between cases and controls, we adjusted for referral pattern to our hospital. Second, as with other case–control studies, this study may suffer from recall bias. Although the questionnaires were completed before the diagnosis in our hospital, in some cases, patients referred from other institutions might have known the diagnosis. Third, we used a self-administered questionnaire to evaluate the nutrients intake, including folate. Data obtained from FFQ may not reflect intake as accurately as those from other methods, such as biological markers. We could not find any association with intake of vitamin C and E or folate for lung cancer risk, contrasting with our previous demonstration using the same population of protective effects of vegetables and fruits (4). The estimation of consumption by FFQ may be one possible explanation for this apparent anomaly. However, the reproducibility and validity of the FFQ were acceptable (28). We could not consider consumption of folate from supplements in total consumption, but the proportion of user with folate supplement is very low in Japan (0.1%) (49). Lastly, the limited number of cases, especially in subanalysis, is another factor and replication of our findings in a larger study is warranted.

In conclusion, we observed significant associations between *MTHFR* C677T and combined *MTHFR* C677T/A1298C polymorphisms and squamous/small cell carcinoma risk among heavy smokers and drinkers. Moreover, interactions between *MTRR* polymorphisms and smoking as well as the *MTHFR* A1298C polymorphism and alcohol consumption were also suggested. Our results thus support the hypothesis that folate metabolism-related gene polymorphisms may play a role in the genesis of lung cancer in combination with environmental factors. Replication in large epidemiological studies as well as studies of the mechanisms of the metabolisms is to be recommended.

Acknowledgements

Authors are grateful to the staff of the Division of Epidemiology and Prevention at Aichi Cancer Center Research Institute for their assistance. The study was supported by a Grant-in-Aid for Scientific Research from the Ministry of Education, Science, Sports, Culture and Technology of Japan and by a Grant-in-Aid for the Third Term Comprehensive 10-Year Strategy for Cancer Control from the Ministry of Health, Labour and Welfare of Japan.

Conflict of Interest statement: None declared.

References

1. Kuroishi,T. *et al.* (2005) Cancer mortality in Japan. In Tajima,K., Kuroishi,T. and Oshima,A. (eds) *Gann Monograph on Cancer Research* Japan Scientific Societies Press, Tokyo, pp. 1–93.
2. Steinmetz,K.A. *et al.* (1991) Vegetables, fruit, and cancer. I. Epidemiology. *Cancer Causes Control*, **2**, 325–357.
3. Steinmetz,K.A. *et al.* (1991) Vegetables, fruit, and cancer. II. Mechanisms. *Cancer Causes Control*, **2**, 427–442.
4. Takezaki,T. *et al.* (2001) Dietary factors and lung cancer risk in Japanese: with special reference to fish consumption and adenocarcinomas. *Br. J. Cancer*, **84**, 1199–1206.
5. Bandera,E.V. *et al.* (1997) Diet and alcohol consumption and lung cancer risk in the New York State Cohort (United States). *Cancer Causes Control*, **8**, 828–840.
6. Voorrips,L.E. *et al.* (2000) A prospective cohort study on antioxidant and folate intake and male lung cancer risk. *Cancer Epidemiol. Biomarkers Prev.*, **9**, 357–365.
7. Shen,H. *et al.* (2003) Dietary folate intake and lung cancer risk in former smokers: a case-control analysis. *Cancer Epidemiol. Biomarkers Prev.*, **12**, 980–986.
8. Duthie,S.J. (1999) Folic acid deficiency and cancer: mechanisms of DNA instability. *Br. Med. Bull.*, **55**, 578–592.
9. Choi,S.W. *et al.* (2000) Folate and carcinogenesis: an integrated scheme. *J. Nutr.*, **130**, 129–132.
10. Wei,Q. *et al.* (2003) Association between low dietary folate intake and suboptimal cellular DNA repair capacity. *Cancer Epidemiol. Biomarkers Prev.*, **12**, 963–969.
11. Bailey,L.B. *et al.* (1999) Polymorphisms of methylenetetrahydrofolate reductase and other enzymes: metabolic significance, risks and impact on folate requirement. *J. Nutr.*, **129**, 919–922.
12. Radparvar,S. *et al.* (1988) Characteristics of thymidylate synthase purified from a human colon adenocarcinoma. *Arch. Biochem. Biophys.*, **260**, 342–350.
13. Leclerc,D. *et al.* (1996) Human methionine synthase: cDNA cloning and identification of mutations in patients of the cblG complementation group of folate/cobalamin disorders. *Hum. Mol. Genet.*, **5**, 1867–1874.
14. Leclerc,D. *et al.* (1998) Cloning and mapping of a cDNA for methionine synthase reductase, a flavoprotein defective in patients with homocystinuria. *Proc. Natl Acad. Sci. USA*, **95**, 3059–3064.
15. Sharp,L. *et al.* (2004) Polymorphisms in genes involved in folate metabolism and colorectal neoplasia: a HuGE review. *Am. J. Epidemiol.*, **159**, 423–443.
16. Shen,H. *et al.* (2001) Polymorphisms of methylene-tetrahydrofolate reductase and risk of lung cancer: a case-control study. *Cancer Epidemiol. Biomarkers Prev.*, **10**, 397–401.
17. Siemianowicz,K. *et al.* (2003) Methylenetetrahydrofolate reductase gene C677T and A1298C polymorphisms in patients with small cell and non-small cell lung cancer. *Oncol. Rep.*, **10**, 1341–1344.
18. Jeng,Y.L. *et al.* (2003) The methylenetetrahydrofolate reductase 677C–>T polymorphism and lung cancer risk in a Chinese population. *Anticancer Res.*, **23**, 5149–5152.
19. Shen,M. *et al.* (2005) Polymorphisms in folate metabolic genes and lung cancer risk in Xuan Wei, China. *Lung Cancer*, **49**, 299–309.
20. Shi,Q. *et al.* (2005) Sex differences in risk of lung cancer associated with methylene-tetrahydrofolate reductase polymorphisms. *Cancer Epidemiol. Biomarkers Prev.*, **14**, 1477–1484.
21. Shi,Q. *et al.* (2005) Polymorphisms of methionine synthase and methionine synthase reductase and risk of lung cancer: a case-control analysis. *Pharmacogenet. Genomics*, **15**, 547–555.
22. Shi,Q. *et al.* (2005) Case-control analysis of thymidylate synthase polymorphisms and risk of lung cancer. *Carcinogenesis*, **26**, 649–656.
23. Tajima,K. *et al.* (2000) A model of practical cancer prevention for outpatients visiting a hospital: the Hospital-based Epidemiologic Research Program at Aichi Cancer Center (HERPACC). *Asian Pac. J. Cancer Prev.*, **1**, 35–47.
24. Hamajima,N. *et al.* (2001) Gene-environment interactions and polymorphism studies of cancer risk in the Hospital-based Epidemiologic Research Program at Aichi Cancer Center II (HERPACC-II). *Asian Pac. J. Cancer Prev.*, **2**, 99–107.
25. Tokudome,S. *et al.* (1998) Development of data-based semi-quantitative food frequency questionnaire for dietary studies in middle-aged Japanese. *Jpn. J. Clin. Oncol.*, **28**, 679–687.
26. Tokudome,S. *et al.* (2004) Development of a data-based short food frequency questionnaire for assessing nutrient intake by middle-aged Japanese. *Asian Pac. J. Cancer Prev.*, **5**, 40–43.
27. Ma,J. *et al.* (1997) Methylenetetrahydrofolate reductase polymorphism, dietary interactions, and risk of colorectal cancer. *Cancer Res.*, **57**, 1098–1102.
28. Tokudome,Y. *et al.* (2005) Relative validity of a short food frequency questionnaire for assessing nutrient intake versus three-day weighed diet records in middle-aged Japanese. *J. Epidemiol.*, **15**, 135–145.
29. Kabat,G.C. *et al.* (1992) Body mass index and lung cancer risk. *Am. J. Epidemiol.*, **135**, 769–774.
30. Heimburger,D.C. *et al.* (1988) Improvement in bronchial squamous metaplasia in smokers treated with folate and vitamin B12. Report of a preliminary randomized, double-blind intervention trial. *JAMA*, **259**, 1525–1530.
31. Saito,M. *et al.* (1994) Chemoprevention effects on bronchial squamous metaplasia by folate and vitamin B12 in heavy smokers. *Chest*, **106**, 496–499.
32. Le Marchand,L. *et al.* (1989) Vegetable consumption and lung cancer risk: a population-based case-control study in Hawaii. *J. Natl Cancer Inst.*, **81**, 1158–1164.
33. Speizer,F.E. *et al.* (1999) Prospective study of smoking, antioxidant intake, and lung cancer in middle-aged women (USA). *Cancer Causes Control*, **10**, 475–482.
34. Hartman,T.J. *et al.* (2001) Association of the B-vitamins pyridoxal 5'-phosphate (B(6)), B(12), and folate with lung cancer risk in older men. *Am. J. Epidemiol.*, **153**, 688–694.
35. Jatoi,A. *et al.* (2001) Folate status among patients with non-small cell lung cancer: a case-control study. *J. Surg. Oncol.*, **77**, 247–252.
36. Frosst,P. *et al.* (1995) A candidate genetic risk factor for vascular disease: a common mutation in methylenetetrahydrofolate reductase. *Nat. Genet.*, **10**, 111–113.
37. Weisberg,I. *et al.* (1998) A second genetic polymorphism in methylenetetrahydrofolate reductase (MTHFR) associated with decreased enzyme activity. *Mol. Genet. Metab.*, **64**, 169–172.
38. van der Put,N.M. *et al.* (1998) A second common mutation in the methylenetetrahydrofolate reductase gene: an additional risk factor for neural-tube defects? *Am. J. Hum. Genet.*, **62**, 1044–1051.
39. Yang,C.X. *et al.* (2005) Gene-environment interactions between alcohol drinking and the MTHFR C677T polymorphism impact on esophageal cancer risk: results of a case-control study in Japan. *Carcinogenesis*, **26**, 1285–1290.
40. Church,D.F. *et al.* (1985) Free-radical chemistry of cigarette smoke and its toxicological implications. *Environ. Health Perspect.*, **64**, 111–126.
41. Mufti,S.I. *et al.* (1993) Alcohol-associated generation of oxygen free radicals and tumor promotion. *Alcohol.*, **28**, 621–628.
42. Halsted,C.H. *et al.* (2002) Metabolic interactions of alcohol and folate. *J. Nutr.*, **132**, 2367S–2372S.
43. Norppa,H. (2004) Cytogenetic biomarkers and genetic polymorphisms. *Toxicol. Lett.*, **149**, 309–334.
44. Zijno,A. *et al.* (2003) Folate status, metabolic genotype, and biomarkers of genotoxicity in healthy subjects. *Carcinogenesis*, **24**, 1097–1103.
45. Bonassi,S. *et al.* (2003) Effect of smoking habit on the frequency of micronuclei in human lymphocytes: results from the Human MicroNucleus project. *Mutat. Res.*, **543**, 155–166.
46. Iarmarcovai,G. *et al.* (2007) Exposure to genotoxic agents, host factors, and lifestyle influence the number of centromeric signals in micronuclei: a pooled re-analysis. *Mutat. Res.*, **615**, 18–27.
47. Inoue,M. *et al.* (1997) Epidemiological features of first-visit outpatients in Japan: comparison with general population and variation by sex, age, and season. *J. Clin. Epidemiol.*, **50**, 69–77.
48. Yoshimura,K. *et al.* (2003) Allele frequencies of single nucleotide polymorphisms (SNPs) in 40 candidate genes for gene-environment studies on cancer: data from population-based Japanese random samples. *J. Hum. Genet.*, **48**, 654–658.
49. Imai,T. *et al.* (2006) Dietary supplement use by community-living population in Japan: data from the National Institute for Longevity Sciences Longitudinal Study of Aging (NILS-LSA). *J. Epidemiol.*, **16**, 249–260.

Received February 19, 2007; revised April 4, 2007; accepted April 21, 2007

Oncogene (2007) 26, 4025–4031

www.nature.com/onc

SHORT COMMUNICATION

CLCP1 interacts with semaphorin 4B and regulates motility of lung cancer cells

H Nagai[1,2,3], N Sugito[2], H Matsubara[1,3], Y Tatematsu[2], T Hida[4], Y Sekido[2], M Nagino[3], Y Nimura[3], T Takahashi[1,2] and H Osada[2]

[1]Division of Molecular Carcinogenesis, Center for Neurological Diseases and Cancer, Nagoya University Graduate School of Medicine, Nagoya, Japan; [2]Division of Molecular Oncology, Aichi Cancer Center Research Institute, Nagoya, Japan; [3]Division of Surgical Oncology, Department of Surgery, Nagoya University Graduate School of Medicine, Nagoya, Japan and [4]Department of Pulmonary Medicine, Aichi Cancer Center Hospital, Nagoya, Japan

We previously established a highly metastatic subline, LNM35, from the NCI-H460 lung cancer cell line, and demonstrated upregulation of a novel gene, *CLCP1* (CUB, LCCL-homology, coagulation factor V/VIII homology domains protein), in LNM35 and lung cancer specimens. In this study, we focused on the potential roles of that gene in cancer metastasis. First, we established stable LNM35 RNAi clones, in which *CLCP1* expression was suppressed by RNAi, and found that their motility was significantly reduced, although growth rates were not changed. Next, *in vitro* selection of a phage display library demonstrated that a phage clone displaying a peptide similar to a sequence within the Sema domain of semaphorin 4B (SEMA4B) interacted with LNM35. Immunoprecipitation experiments confirmed interaction of CLCP1 with SEMA4B, regulation of CLCP1 protein by ubiquitination and proteasome degradation enhanced in the presence of SEMA4B. These results are the first to indicate that CLCP1 plays a role in cell motility, whereas they also showed that at least one of its ligands is SEMA4B and that their interaction mediates proteasome degradation by CLCP1. Although the physiological role of the interaction between CLCP1 and SEMA4B remains to be investigated, this novel gene may become a target of therapy to inhibit metastasis of lung cancers.
Oncogene (2007) **26,** 4025–4031; doi:10.1038/sj.onc.1210183; published online 8 January 2007

Keywords: CLCP1; SEMA4B; lung cancer

Lung cancer is the leading cause of cancer-related death in developed countries. Despite a considerable body of knowledge regarding the molecular mechanisms of development and progression of lung cancer, most patients eventually die because of widespread metastases. Thus, it is considered important to identify the molecules that play crucial roles in cell motility/invasion and metastasis in order to significantly reduce mortality rates. For this purpose, we established a highly metastatic subline, LNM35, from the NCI-H460 human lung cancer cell line (Kozaki *et al.*, 2000), which showed upregulation of various proinflammatory cytokines and angiogenic chemotactic chemokines in comparison to a representative low metastatic clone of the parental line (Kozaki *et al.*, 2001). Based on this profiling analysis, we also identified and characterized a novel gene, *CLCP1* (CUB, LCCL-homology, coagulation factor V/VIII homology domains protein), also termed endothelial and smooth muscle cell-derived neuropilin-like molecule (*ESDN*)/discoidin, CUB and LCCL domain containing 2 (*DCBLD2*) (Kobuke *et al.*, 2001), that demonstrated upregulated expression in LNM35 as well as in a significant fraction of lung cancers, especially lymph node metastases (Koshikawa *et al.*, 2002). The *CLCP1* gene encodes a 775-amino-acid protein with structural similarities to neuropilins, cell surface receptors for vascular endothelial growth factor $(VEGF)_{165}$ and semaphorins (Koshikawa *et al.*, 2002), which were originally identified as neural axon repulsion signaling molecules active in axon guidance. Some class III semaphorins function as tumor suppressors, whereas one class IV member may promote tumor progression through induction of angiogenesis (Kruger *et al.*, 2005). In the present study, we explored the functions of CLCP1 in tumor progression and metastasis, and found that knock down reduces tumor cell motility. Using the phage peptide library, we also obtained evidence that at least one ligand of CLCP1, Sema domain of the human semaphorin 4B (SEMA4B), is a class IV semaphorin that may be also involved in the regulation of cell motility through its induction of CLCP1 degradation.

Observation of a high expression of *CLCP1* in lung cancer specimens prompted us to examine its functional contribution to the high metastatic properties of LNM35 cells. We generated several small interfering RNA (siRNA) constructs expressing short hairpin RNAs targeting CLCP1, and found two siRNA sites (siCLCP1–2 and siCLCP1–3) that were able to effectively knock down CLCP1 expression in 293T cells co-transfected with a CLCP1 expression vector and an

Correspondence: Dr H Osada, Division of Molecular Oncology, Aichi Cancer Center Research Institute, 1-1 Kanokoden, Chikusa-ku, Nagoya 464-8681, Japan.
E-mail: hosada@aichi-cc.jp
Received 5 June 2006; revised 30 October 2006; accepted 2 November 2006; published online 8 January 2007

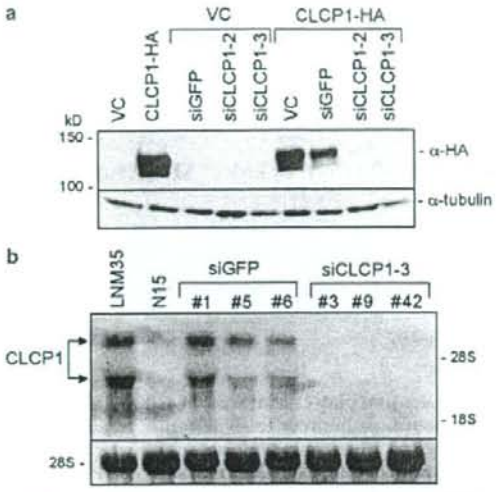

Figure 1 CLCP1 expression and establishment of LNM35-RNAi clones. (**a**) Immunoblotting of CLCP1-RNAi transfectants. RNAi plasmid vectors were constructed by insertion of the H1 promoter 5′ upstream of the CMV promoter driving a neomycin-resistant gene (pH1-RNA neomycin). CLCP1-RNAi sites were designed at 1196–1214 nt and 1935–1953 nt of *CLCP1* ORFs for siCLCP1–2 and siCLCP1–3, respectively. A blast homology search did not indicate any strong homology for these RNAi sites. 293T cells were transfected with each RNAi-vector along with the HA-tagged CLCP1 expression vector (Koshikawa *et al*., 2002). A control RNAi construct for the GFP gene, siGFP, was also used. Note the significant reduction of expression of CLCP1 protein observed with siCLCP1–2 and siCLCP1–3. (**b**) Northern blotting of stable LNM35-RNAi clones. LNM35 was transfected with siCLCP1–3 RNAi constructs and selected with neomycin (1 mg/ml) for 2 weeks. The expression of endogenous *CLCP1* transcripts was almost undetectable in the LNM35 siCLCP1–3 clones (nos. 3, 9 and 42), whereas the high level of expression of *CLCP1* was not affected in control clones that received the siGFP construct. Note the significant difference in *CLCP1* expression level between LNM35 and the parental line N15.

siRNA vector (Figure 1a). To determine whether these findings were associated with decreased cell growth and/or motility of LNM35, we established stable LNM35 transfectant clones. Northern blotting (Figure 1b) revealed that the expression level of *CLCP1* in siCLCP1–3 clones nos. 3, 9 and 42 was significantly reduced to the level of the parental subclone of NCI-H460, N15, whereas *CLCP1* expression was not affected in control siGreen fluorescent protein (siGFP) clones (Supplementary Figure 3). Thereafter, these three siCLCP1–3 clones were employed for further biological analyses.

Cell growth rate was studied and the growth rates of the siCLCP1–3 clones were quite similar to those of siGFP clones (Figure 2a), suggesting that CLCP1 expression is not involved in the regulation of cell growth in LNM35 cells. However, motility was significantly decreased in the siCLCP1–3 clones, whereas the siGFP clones retained high motility (Figure 2b and c), implying that CLCP1 has an effect to enhance cell migration.

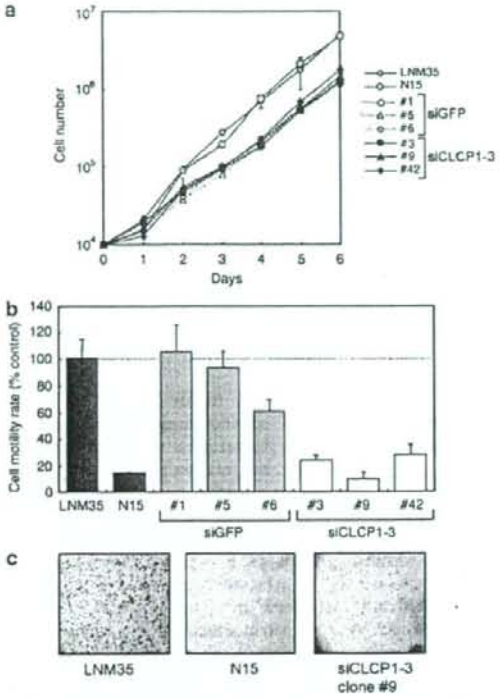

Figure 2 Cell proliferation and motility of LNM35 RNAi clones. (**a**) Cell proliferation assay. Stable clones were plated at 1×10^4 per dish in RPMI1640 medium with 5% fetal bovine serum and neomycin, then cell numbers were counted each day with a Z1 Coulter Counter (Beckman Coulter, Fullerton, CA, USA). The growth rates of the siCLCP1–3 clones were quite similar to those of the control siGFP clones, (**b**, **c**) *in vitro* motility assay. Motility of the RNAi clones was studied using transwell chambers, as described previously (Kozaki *et al*., 2001) and found to be significantly decreased in all three siCLCP1–3 clones (white bars), whereas the siGFP clones (hatched bars) retained their high levels of motility. (**c**) A number of migrated cells were observed among the LNM35 cells by Giemsa staining, whereas there were very few N15 or siCLCP1 cells (× 40 magnification). The small dots represent 8 μm-sized transwell chamber pores.

Concurrently with the above analyses, we searched for cell surface molecules specific to LNM35 using a phage display method in order to identify the molecular mechanisms of the high motility/invasion ability of LNM35. One of the peptides enriched with this method was SAYIPDS, whose sequence was nearly identical to that of SAYIPES within the SEMA4B gene (Figure 3a). This domain is known to be crucial for interactions with other proteins. CLCP1 has structural similarities to neuropilins, which function as cell surface receptors for semaphorins, therefore, we speculated that the selected peptide and SEMA4B might interact with CLCP1. We compared the interactions of the phage with LNM35 (high CLCP1 expression) and N15 (low CLCP1 expression). When cells were incubated with the phage displaying the

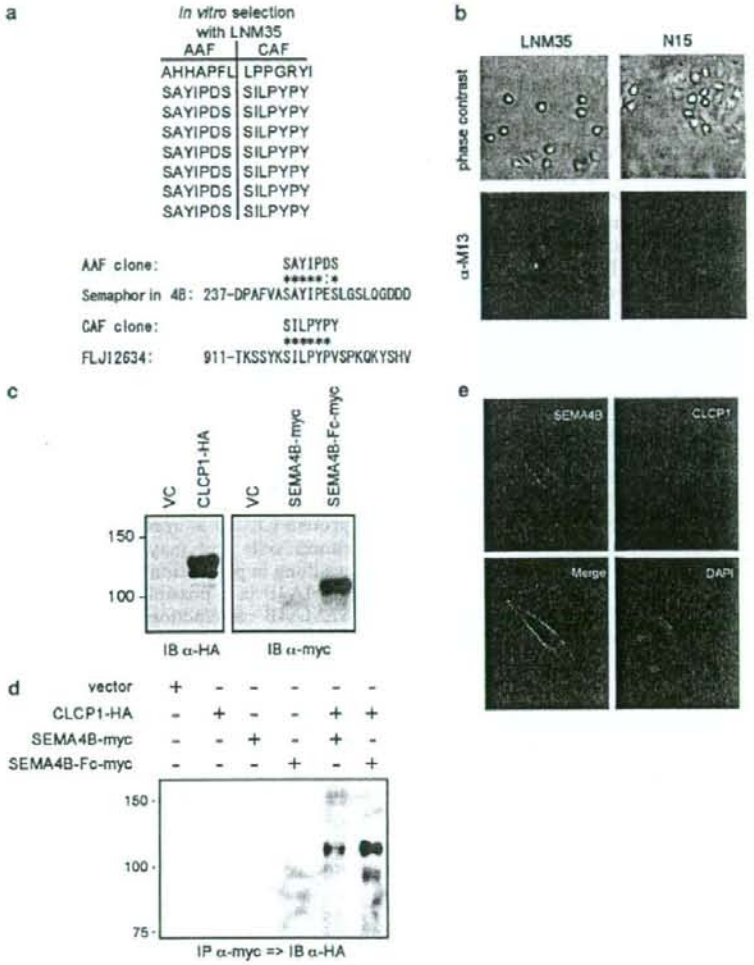

Figure 3 CLCP1 interacts with SEMA4B. (**a**) *In vitro* selection of LNM35 cells using a phage display library (PhD-7 Phage Display Peptide Library, New England Biolabs, Ipswich, MA, USA). For each selection, $1–2 \times 10^{11}$ PFU of phage particles were overlaid on LNM35 cells. After incubation and washing, attached phages were eluted with acid elution buffer (acid-associated fraction (AAF)). Tightly associated phages were also recovered after cell lysis (cell-associated fraction (CAF)). The phages were amplified following infection with bacteria and rounds of incubation-elution-amplification were repeated. Seven of the eight AAF phage clones sequenced after four rounds of selection contained the SAYIPDS peptide, which was nearly identical to the sequence SAYIPES within the SEMA4B gene. CAF phage results indicated the sequence of a hypothetical protein FLJ12634. (**b**) Immunofluorescence of phages attached to LNM35. Both LNM35 (with high CLCP1 expression) and N15 (with low CLCP1 expression) cells were incubated with phages displaying the SAYIPDS peptide. After washing and fixation, cell-attached phages were immuno-stained with the monoclonal antibody against M13 procoat protein (GE Healthcare Bio-Science, Piscataway, NJ, USA) and Alexa488-conjugated anti-mouse IgG (Invitrogen, Carlsbad, CA, USA). Note the stronger binding of the SAYIPDS phage with LNM35 as compared to that with N15. (**c**, **d**) Co-immunoprecipitation of CLCP1 with SEMA4B. The SEMA4B cDNA clone, KIAA1745, was kindly provided by Kazusa DNA Research Institute. For the SEMA4B-myc expression construct, the SEMA4B ORF was introduced into pcDNA3 (Invitrogen) together with myc-tag at its C-terminus. For the SEMA4B-Fc-myc construct, a 1720-bp *Sac*II-*Bam*HI fragment of KIAA1745 containing only the Sema domain was fused to the cDNA of the human IgG1 Fc portion in the pcDNA vector with an myc-tag at the C-terminus of the Fc portion. SEMA4B-myc or SEMA4B-Fc-myc was co-transfected with CLCP1-HA into 293T cells, and the generated proteins were immunoprecipitated with mouse monoclonal anti-myc-tag antibody 9E10. Immunoblots of these precipitates with rabbit anti-HA antibodies clearly demonstrated co-immunoprecipitation of CLCP1 with SEMA4B proteins. (**e**) Immunofluorescence of SEMA4B and CLCP1. The A549 lung cancer cell line was transfected with SEMA4B-myc and CLCP1-HA expression vectors, then stained with Alexa Fluor dye-labeled secondary antibodies (Invitrogen) after MG-132 treatment, as performed in Figure 4b and c. Observation with a confocal microscope (Olympus, Tokyo, Japan) showed both CLCP1 and SEMA4B to be mainly localized on the cell surface membrane, with colocalization clearly observed in merged images.

SAYIPDS peptide and then immuno-stained with the anti-M13 antibody against the phage particle, LNM35 staining was more intense than that of N15 (Figure 3b). Next, the indicated interaction between CLCP1 and SEMA4B was studied using an myc-tagged full-length SEMA4B construct, as well as an myc-tagged SEMA4B-Fc fusion construct consisting of the SEMA4B Sema domain and immunoglobulin (Ig)G Fc portion. After co-transfection with hemagglutinin (HA)-CLCP1 into 293T cells, anti-HA immunoblotting of anti-myc immunoprecipitates clearly demonstrated co-precipitation of CLCP1 with SEMA4B or SEMA4B-Fc (Figure 3d). Further, colocalization of CLCP1 and SEMA4B proteins on cell surface membranes was demonstrated by immunofluorescence analysis (Figure 3e).

HA-tagged CLCP1 demonstrated two sizes, 130 and 110 kDa, which were both larger than the predicted molecular mass of 80 kDa. We previously speculated that post-translational modifications such as glycosylation might account for this discrepancy (Koshikawa *et al*., 2002), as is the case with most transmembrane proteins. To confirm this, 293T cells were transfected with HA-CLCP1 and then treated with tunicamycin, which blocks the first step in the biosynthesis of N-linked oligosaccharides. Tunicamycin treatment reduced the amounts of both the 130- and 110-kDa bands in a dose-dependent manner. Simultaneously, a novel 80-kDa band appeared (Figure 4a), indicating that CLCP1 protein is indeed post-translationally modified by glycosylation, resulting in 130- and 110-kDa-sized proteins, which might be properly processed into transmembrane proteins.

We found that the intensity of the CLCP1 protein band was significantly weaker after CLCP1-SEMA4B co-transfection as compared to with CLCP1 transfection alone (Figure 4b), and subsequently attempted to determine whether SEMA4B caused degradation of CLCP1 protein in a proteasome-dependent manner. When 293T cells were transfected with CLCP1 and/or SEMA4B, and then treated with MG-132, a specific inhibitor of proteasomes, anti-HA immunoblots indicated an increased intensity of both the 130- and 110-kDa bands in the CLCP1 transfectants (Figure 4b, lanes 3 and 4), suggesting that CLCP1 alone was originally regulated by proteasome degradation. However, CLCP1–SEMA4B and CLCP1–SEMA4B-Fc co-transfection were both associated with a significantly reduced intensity of the largest band (130 kDa) (Figure 4b, lanes 5 and 7). Similarly, MG-132 treatment enhanced the intensity of the 110-kDa band (Figure 4b, lanes 4, 6 and 8). However, the 130-kDa band was only moderately restored with CLCP1–SEMA4B co-transfection (Figure 4b, lane 6) and not recovered at all with CLCP1–SEMA4B-Fc co-transfection (Figure 4b, lane 8). In Figure 4c, the size of the co-immunoprecipitated CLCP1 isoform was compared with that of CLCP1 proteins in cell lysates derived from transfectants treated with or without MG-132 or another proteasome inhibitor, lactacystin, which was effective for a Smad4 mutant (Yanagisawa *et al*., 2000) (Supplementary Figures 1 and 2). The main co-precipitated CLCP1 isoform appeared to be a 110-kDa isoform, even in samples treated with proteasome inhibitors. These findings suggest that the degradation of the 130-kDa band induced by SEMA4B proteins may be too severe to be inhibited by the applied concentration of MG-132. Nevertheless, even with higher concentrations of proteasome inhibitors, full restoration of the 130-kDa band was not obtained (Supplementary Figure 2), suggesting that the interactions with SEMA4B proteins, especially SEMA4B-Fc, may not only induce degradation, but also affect full glycosylation of CLCP1. We also examined the ubiquitination status of CLCP1 using P4D1 monoclonal antibodies that recognize both monoUb and polyUb (Figure 4d). Although ubiquitinated CLCP1 was readily detected in cells co-transfected with the empty vector (Figure 4d, lane 4), the ubiquitination of CLCP1 was significantly increased following co-transfection with SEMA4B (Figure 4d, lane 6). These results suggest that CLCP1–SEMA4B interactions induce significant degradation of CLCP1 proteins, especially 130-kDa fully-glycosylated CLCP1.

This present results indicated that the neuropilin-like protein CLCP1 is upregulated in highly metastatic lung cancer cells and may promote cell motility, possibly resulting in promotion of metastasis. We also found that SEMA4B is a possible ligand of CLCP1, as CLCP1–SEMA4B interaction caused CLCP1 degradation. CLCP1/ESDN was also reported to be expressed by vascular smooth muscle cells, as well as upregulated by platelet-derived growth factor-BB stimulation and vascular injury, suggesting that it modulates growth-promoting signals (Kobuke *et al*., 2001). Class III semaphorins interact with neuropilins through binding of their Sema and CUB or FV/VIII domains, respectively. Although the interaction domains of CLCP1 and SEMA4B have yet to be determined, it is conceivable that the Sema domain of SEMA4B interacts with CUB and FV/VIII domains of CLCP1. The fact that the sequence within the Sema domain was enriched with the phage display selection in LNM35 expressing CLCP1 provides support for this speculation.

Cell migration is a multistep process that includes leading edge protrusion, focal contact formation and actomyosin-dependent cell contraction, and also involves small guanosine triphosphatase (GTPase) and integrins. Small GTPases, including Rho, Rac and Cdc42, control cell motility by regulating actin and microtubule dynamics (Friedl and Wolf, 2003). Semaphorins and neuropilins make protein complexes with plexins, which regulate the activities of small GTPases through interactions with these small GTPases and Rho-guanine nucleotide exchange factor (Kruger *et al*., 2005). In addition, a recent report showed that Sema4D-plexin-B1 interaction downregulates R-Ras activity through the endogenous GTPase-activating protein activity of plexin-B1, resulting in inhibition of focal contact mediated by integrins (Oinuma *et al*., 2004). Therefore, to understand the molecular mechanisms underlying the regulation of cell motility by CLCP1, it is important to clarify whether CLCP1 signaling has any effects on the activities of these small GTPases and integrins.

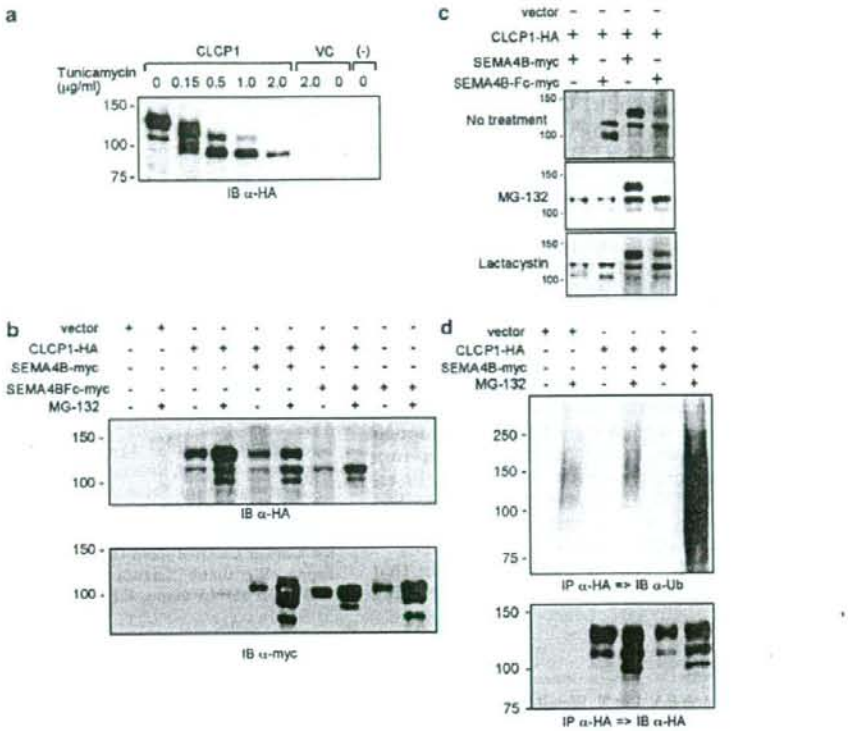

Figure 4 Post-translational modification of CLCP1 protein. (**a**) *N*-glycosylation of CLCP1. 293T cells were transfected with the CLCP1-HA vector and then treated with an *N*-linked glycosylation inhibitor, tunicamycin (Wako Pure Chemical Industries Ltd., Osaka, Japan), for 24 h at the indicated concentrations. Reductions in the amounts of both the 130- and 110-kDa bands resulted, with simultaneous appearance of a novel 90-kDa band similar to the predicted size in a dose-dependent manner. (**b**) Degradation of CLCP1 protein. 293T cells were transfected with CLCP1-HA, SEMA4B-myc and/or SEMA4B-Fc-myc, then treated with a proteasome inhibitor, MG-132 (SIGMA-ALDRICH, St Louis, MO, USA), at 10 μM for 24 h. The expression levels of CLCP1 and SEMA4B proteins were then investigated using anti-HA and anti-myc antibodies. Without MG-132 treatment, the CLCP1 protein band was significantly weaker after CLCP1/SEMA4B or CLCP1/SEMA4B-Fc co-transfection (lanes 5, 7) than with CLCP1 transfection alone (lane 3). MG-132 treatment enhanced the intensity of the CLCP1 protein band in co-transfections (lanes 6, 8) and also with CLCP1 transfection alone (lane 4). Proteasome-dependent degradations of SEMA4B proteins were also observed. (**c**) Analysis of the co-immunoprecipitated isoform of CLCP1. Immunoprecipitation and immunoblotting of CLCP1/SEMA4B and CLCP1/SEMA4B-Fc co-transfected cells were conducted, the same as in Figure 3d. Transfected cells were treated with MG-132 (10 μM) or another proteasome inhibitor, lactacystin (15 μM, Wako Pure Chemical Industries Ltd.). Immunoprecipitated proteins (lane 1, 2) were run with cell lysates before immunoprecipitation (lane 3, 4). The main immunoprecipitated CLCP1 isoform appeared to be the same 110-kDa isoform noted in (**a**). (**d**) Ubiquitination of CLCP1. As in (b), 293T cells were transfected and treated with MG-132. Then, CLCP1 protein was immunoprecipitated with the anti-HA antibody and analysed with the anti-ubiquitin antibody, P4D1 (Santa Cruz Biotechnology, Inc., Santa Cruz, CA, USA). Ubiquitination of CLCP1 was readily detected following transfection of CLCP1 alone (lane 4) and significantly increased by co-transfection with SEMA4B (lane 6).

In a previous study, SEMA3A inhibited the migration and spread of a breast cancer cell line, MDA-MB-231, which expresses neuropilin-1 and plexin-A1, whereas another ligand of neuropilin-1, $VEGF_{165}$, was shown to compete with SEMA3A and abrogate its inhibitory effect (Bachelder *et al*., 2003). CLCP1 may also interact with other ligand molecules, which might regulate cell motility in competition with SEMA4B. In the present study, we also examined the involvement of cyclooxygenase 2 (COX-2) in *CLCP1* expression (Supplementary Figure 4), because a previous study showed that COX-2 was upregulated in LNM35 cells and contributed to their highly metastatic characteristics (Kozaki *et al*., 2000). We found that nimesulide, a COX-2 inhibitor, repressed *CLCP1* mRNA levels, suggesting a functional association between COX-2 activation and *CLCP1* overexpression in LNM35 cells.

SEMA3B and *SEMA3F*, which are localized at the 3p21.3 locus, are frequently deleted in lung cancers and have been found to suppress tumor cell proliferation (Tse *et al*., 2002; Xiang *et al*., 2002; Castro-Rivera *et al*., 2004). In contrast, class IV semaphorins do not show

such a tumor suppressor function, whereas Sema4D was originally reported to promote B-cell survival and T-cell activation. Another study showed that Sema4D induces angiogenesis, which was mediated by the coupling of its high-affinity receptor plexin-B1 with the Met tyrosine kinase (Conrotto *et al*., 2005). In addition, class IV semaphorins frequently have PDZ {PSD (postsynaptic density protein) 95, DlgA (Discs large A), and ZO (zonula occludens) 1)} domain-binding motifs at their C-termini, through which they may function as receptors by mediating signal transfers through their intracellular domains. SEMA4B, 4C and 4F have been shown to interact with the PDZ domains of PSD-95 (Inagaki *et al*., 2001; Burkhardt *et al*., 2005), whereas SEMA4D was found to associate with CD45 protein tyrosine phosphatase (Herold *et al*., 1996). Therefore, SEMA4B might function as a CLCP1 receptor. Sema3A–neuropilin interactions induce neuropilin-1 endocytosis, which is mediated by L1-CAM (Fournier *et al*., 2000; Castellani *et al*., 2004), which in turn modulates growth cone sensitivity to semaphorin repulsion signals. CLCP1 degradation after CLCP1–SEMA4B interaction may indicate an induction of CLCP1 endocytosis by SEMA4B.

In conclusion, the present results indicate that CLCP1 and its interactions with ligands including SEMA4B may become molecular targets for therapeutic inhibition of metastasis. In addition to CLCP1-siRNA, the suppression of CLCP1 functions with dominant-negative CLCP1 or negatively regulating ligands might inhibit *in vitro* motility and, consequently, *in vivo* metastasis of cancer cells. Fine mapping of the interacting regions between CLCP1 and SEMA4B may indicate concrete molecular targets. Although a full understanding of the biological roles of CLCP1 and SEMA4B remains to be achieved, further investigations of CLCP1 functions should provide novel and useful strategies to improve the clinical prognosis of lung cancer patients by facilitating the suppression of metastasis.

Acknowledgements

This work was supported in part by a Grant-in-Aid for Scientific Research on Priority Areas from the Ministry of Education, Culture, Sports, Science and Technology of Japan, a Grant-in-Aid for Scientific Research (B) and (C) from the Japan Society for the Promotion of Science, and a Grant-in-Aid for the Second Term Comprehensive Ten-Year Strategy for Cancer Control from the Ministry of Health and Welfare, Japan. We thank Kazusa DNA Research Institute for the SEMA4B cDNA clone, KIAA1745.

References

Bachelder RE, Lipscomb EA, Lin X, Wendt MA, Chadborn NH, Eickholt BJ *et al*. (2003). Competing autocrine pathways involving alternative neuropilin-1 ligands regulate chemotaxis of carcinoma cells. *Cancer Res* **63**: 5230–5233.

Burkhardt C, Muller M, Badde A, Garner CC, Gundelfinger ED, Puschel AW. (2005). Semaphorin 4B interacts with the post-synaptic density protein PSD-95/SAP90 and is recruited to synapses through a C-terminal PDZ-binding motif. *FEBS Lett* **579**: 3821–3828.

Castellani V, Falk J, Rougon G. (2004). Semaphorin3A-induced receptor endocytosis during axon guidance responses is mediated by L1 CAM. *Mol Cell Neurosci* **26**: 89–100.

Castro-Rivera E, Ran S, Thorpe P, Minna JD. (2004). Semaphorin 3B (SEMA3B) induces apoptosis in lung and breast cancer, whereas VEGF165 antagonizes this effect. *Proc Natl Acad Sci USA* **101**: 11432–11437.

Conrotto P, Valdembri D, Corso S, Serini G, Tamagnone L, Comoglio PM *et al*. (2005). Sema4D induces angiogenesis through Met recruitment by Plexin B1. *Blood* **105**: 4321–4329.

Fournier AE, Nakamura F, Kawamoto S, Goshima Y, Kalb RG, Strittmatter SM. (2000). Semaphorin3A enhances endocytosis at sites of receptor-F-actin colocalization during growth cone collapse. *J Cell Biol* **149**: 411–422.

Friedl P, Wolf K. (2003). Tumour-cell invasion and migration: diversity and escape mechanisms. *Nat Rev Cancer* **3**: 362–374.

Herold C, Elhabazi A, Bismuth G, Bensussan A, Boumsell L. (1996). CD100 is associated with CD45 at the surface of human T lymphocytes. Role in T cell homotypic adhesion. *J Immunol* **157**: 5262–5268.

Inagaki S, Ohoka Y, Sugimoto H, Fujioka S, Amazaki M, Kurinami H *et al*. (2001). Sema4c, a transmembrane semaphorin, interacts with a post-synaptic density protein, PSD-95. *J Biol Chem* **276**: 9174–9181.

Kobuke K, Furukawa Y, Sugai M, Tanigaki K, Ohashi N, Matsumori A *et al*. (2001). ESDN, a novel neuropilin-like membrane protein cloned from vascular cells with the longest secretory signal sequence among eukaryotes, is up-regulated after vascular injury. *J Biol Chem* **276**: 34105–34114.

Koshikawa K, Osada H, Kozaki K, Konishi H, Masuda A, Tatematsu Y *et al*. (2002). Significant up-regulation of a novel gene, CLCP1, in a highly metastatic lung cancer subline as well as in lung cancers *in vivo*. *Oncogene* **21**: 2822–2828.

Kozaki K, Koshikawa K, Tatematsu Y, Miyaishi O, Saito H, Hida T *et al*. (2001). Multi-faceted analyses of a highly metastatic human lung cancer cell line NCI-H460-LNM35 suggest mimicry of inflammatory cells in metastasis. *Oncogene* **20**: 4228–4234.

Kozaki K, Miyaishi O, Tsukamoto T, Tatematsu Y, Hida T, Takahashi T *et al*. (2000). Establishment and characterization of a human lung cancer cell line NCI-H460-LNM35 with consistent lymphogenous metastasis via both subcutaneous and orthotopic propagation. *Cancer Res* **60**: 2535–2540.

Kruger RP, Aurandt J, Guan KL. (2005). Semaphorins command cells to move. *Nat Rev Mol Cell Biol* **6**: 789–800.

Oinuma I, Ishikawa Y, Katoh H, Negishi M. (2004). The Semaphorin 4D receptor Plexin-B1 is a GTPase activating protein for R-Ras. *Science* **305**: 862–865.

Osada H, Tatematsu Y, Saito H, Yatabe Y, Mitsudomi T, Takahashi T. (2004). Reduced expression of class II histone deacetylase genes is associated with poor prognosis in lung cancer patients. *Int J Cancer* **112**: 26–32.